NACA RM E55F28

NACA

RESEARCH MEMORANDUM

INVESTIGATION OF IMPULSE-TYPE SUPERSONIC COMPRESSOR WITH HUB-TIP RATIO OF 0.6 AND TURNING TO AXIAL DIRECTION

II - STAGE PERFORMANCE WITH THREE DIFFERENT SETS OF STATORS

By Ward W. Wilcox

Lewis Flight Propulsion Laboratory
Cleveland, Ohio

NATIONAL ADVISORY COMMITTEE FOR AERONAUTICS

WASHINGTON

August 16, 1955
Declassified June 24, 1958

NATIONAL ADVISORY COMMITTEE FOR AERONAUTICS

RESEARCH MEMORANDUM

INVESTIGATION OF IMPULSE-TYPE SUPERSONIC COMPRESSOR WITH HUB-TIP RATIO OF 0.6 AND TURNING TO AXIAL DIRECTION

II - STAGE PERFORMANCE WITH THREE DIFFERENT SETS OF STATORS

By Ward W. Wilcox

SUMMARY

An impulse-type supersonic compressor designed for turning to the axial direction was tested in air with three different sets of stator blades at eight angle settings. Although the performance of the rotor alone was good, its combination with stators resulted in a severe reduction in range of weight flow and low values of over-all pressure ratio and adiabatic efficiency.

In the range of stator-inlet relative Mach numbers studied (i.e., 1.4 or less), most of the losses occur as a result of secondary flows, friction, and mixing of the nonuniform Mach number and energy levels that come from the rotor. These results indicate that, in addition to good over-all performance, the rotor must deliver air with nearly uniform stator-entrance conditions (total-pressure ratio and efficiency) and small end-region boundary layers before satisfactory stage performance can be attained.

INTRODUCTION

Although the development of impulse-type supersonic-compressor rotors has progressed to the point where high over-all pressure ratios are obtained at relatively high adiabatic efficiency, efficient diffusion of the high outlet velocity is necessary for satisfactory stage performance. (Impulse-type denotes little or no static-pressure rise in the rotor, thus postponing most of the diffusion to the stator.) In early work, such as reference 1, there was optimism about the ease of diffusion from Mach numbers as high as 2.5. For instance, it was stated that stage pressure ratios between 6 and 10 could be obtained with adiabatic efficiencies between 70 and 80 percent. This work was based on analytical relations and a limited amount of cascade testing. In the cascades, which were two-dimensional in nature, inlet flow was uniform as to direction and Mach

number, and the wall boundary layers were usually removed before the stator entrance. In addition, variable geometry was sometimes employed to improve the flow conditions after starting.

Reference 2 indicated that the application of two-dimensional stators (designed according to the method of characteristics for an inlet Mach number of 1.79) to an impulse-type rotor was rather disappointing. Application of stators at design rotor speed reduced total-pressure ratio from 3.2 to 2.7 for a ratio or "recovery factor" of about 0.85 at inlet Mach number of 1.6. These test results, which were obtained in Freon-12, showed a large increase in total-pressure loss with increasing inlet relative Mach number. The same observation was made in reference 3 for a set of stators designed for an inlet Mach number of 1.8 at a higher inlet flow angle. The recovery factor of these stators at Mach 1.8 was 0.56.

During tests of a rotor that turned to the axial direction at all radii (ref. 4) it was found possible to stabilize a shock in the rear part of the rotor itself, thus departing from true impulse-type operation. Under this type of operation the rotor-outlet Mach number was reduced considerably without drastic reduction of the adiabatic efficiency. For instance, near design speed, Mach number could be reduced from 1.9 to 1.5 with the change in pressure ratio from 5.6 to 5.25 (ref. 5). As reported in reference 5, for stators in which pressure recovery decreases rapidly at high Mach numbers, the optimum match point between the rotor and its stator would be at a rotor-outlet Mach number (as well as pressure ratio and rotor efficiency) lower than that obtained at the highest pressure ratio and efficiency of the rotor alone.

The rotor used in the present investigation, the performance of which was reported in reference 6, was similar to that just discussed, in that the turning was to the axial direction and that it was possible to obtain considerable deceleration within the rotor. This 16-inch-diameter rotor, however, was designed for a lower tip speed of 1400 feet per second, had inlet guide vanes and an inlet hub-tip ratio of 0.6, and was stressed to operate in air. (Previous rotors were designed for 1600-ft/sec tip speed and were tested in Freon-12.) As reported in reference 6, the rotor performance at 90-percent design speed had a peak pressure ratio of 3.7 at an adiabatic efficiency of 0.86. For stator work the average outlet Mach number of 1.4 appeared to present less difficulty than the higher Mach numbers of references 2 and 3.

Two sets of high-solidity supersonic stators were designed, and one set of existing double-circular-arc stators was modified for these tests. In an effort to determine the source of the stator losses, a 26-tube total-pressure rake was used to determine pressure at 182 points behind a single blade channel, and 20 static taps were placed on the opposing pressure and suction surfaces of two adjacent blades. All tests were conducted in air at the NACA Lewis laboratory.

APPARATUS

The apparatus used for the tests reported herein was exactly the same as that for reference 6, except for the stators and the inner fairing behind the rotor. A schematic sketch of the installation is given in figure 1. As shown in figures 1 and 2(a), a straight cylindrical fairing was used for the first series of tests, and a double conical fairing piece was added later. Instrument stations used are numbered in these figures consistently with reference 6. The three sets of stators are discussed separately, and the design detail is presented at the beginning of each section.

INSTRUMENTATION

At station 5, between the rotor and stators, the same types of instruments used and illustrated in reference 6 were used. At station 7, in addition to two split-shield thermocouples and a claw-type yaw probe, a 26-tube total-pressure rake was mounted. This rake had 0.040-inch-diameter tubes on 0.1-inch centers at an angle of 9° with the compressor axis. The tubes were on an arc conforming to the mean radius. Radial surveys were made with each instrument. All instruments were calibrated over a full range of Mach number and pressure level in a separate facility.

In addition to the wall static taps at the measuring stations, a row of taps was placed on the outside wall at 1/2-inch axial intervals, along the centerline of the original passage formed by two blades of the first configuration. The location of these taps is given in figure 2(a). On the surface of two adjacent blades, at the pitch line, ten static taps were installed on the pressure and suction surfaces at 1/2-inch axial intervals (fig. 2(a)).

PROCEDURE

Experimental

With outlet throttles wide open to the laboratory exhaust system, the desired equivalent speed was set. Back pressure was increased by throttling in the collector until audible surging occurred. Test points were taken at each speed to cover the weight-flow range from open throttle to surge. Because of the effect of the instruments on back pressure, it was necessary to run each survey separately with all other instruments drawn up to the wall.

Calculation

All readings of temperature, total pressure, and static pressure were corrected for Mach number and total-pressure-level effects, as applicable, in a conventional manner. The individual readings from the 26-tube total-pressure rake were averaged arithmetically at each radial station, and these values were mass-weighted in the radial direction to obtain a single outlet pressure. Static pressure was assumed to be uniform in the circumferential direction at the rear measuring station 7. All performance parameters are corrected to standard sea-level conditions.

In order to make valid comparisons of over-all adiabatic efficiency and pressure recovery for the various blade settings and configurations, it was necessary to avoid masking the effect of the configuration change by random scatter of data. As shown in figure 3, the station 5 pressure ratios from the stator tests agreed with data from rotor tests within the same scatter band. The effect of blade resettings was frequently small and often of the same magnitude as these deviations from the average. Similarly, measurements of Mach number and energy addition were subject to random error. In order to minimize the effect of such variations and to allow comparisons from blade to blade and setting to setting, consistent values of rotor-outlet pressure ratio and Mach number were established, since addition of the stators appeared to have very little effect on performance at the rotor discharge. Each parameter was plotted against inlet equivalent weight flow for a large number of data points, and a smooth curve was faired through the points. The values from these curves were used for average stator-inlet conditions at the measured rotor-inlet equivalent weight flow.

Because of the large amount of mixing and secondary flows, large circumferential variations of temperature were observed at station 7. In order to get more representative values of $(T_7 - T_0)/T_0$ for efficiency comparisons, it was necessary to use a faired curve based on temperature data at station 7 from the rotor tests. As shown in figure 4, the values used were generally higher than the scattered values obtained with stators installed. For this reason, the efficiencies presented are considered conservative and fair.

RESULTS AND DISCUSSION

Results of the tests of the three sets of stators are presented separately. The various stator configurations are compared in passing, and some general observations are made in a separate section. First, however, it seems desirable to present the flow conditions at the stator entrance for weight flows near the design point. Station 5 data from tests of the rotor alone were used for stator design. For reference purposes, the rotor characteristic maps (i.e., pressure ratio and adiabatic efficiency

against equivalent weight flow) are given in figure 3. As shown in figure 3, pressure ratios observed at station 5 with stators installed fall along the curves determined in tests of the rotor alone.

A more detailed picture of stator-entrance flow is shown in figure 5; that is, the radial variations of Mach number, pressure ratio, flow angle, and energy addition are given for weight flows near the stator design point. Two test points from the station 5 measurements with stators installed are included. A fairly uniform variation in flow angle of about 11° to 14° exists from hub to tip. Further, there is a shift of about 5° for the range of weight flow covered. The radial variation of absolute Mach number shows fairly good agreement between the rotor-alone case and the case where stators are installed. However, the actual variation of Mach number is nonuniform and varies considerably with inlet weight flow. The trends exhibited by the total-pressure ratio at station 5 are virtually the same as for the absolute Mach number. As stated in the design section of reference 6 in specifying radial-element blades and turning to the axial direction at all radii, a radial gradient of energy addition is set up at the rotor exit. The actual energy addition is shown in figure 5 as a plot of temperature rise divided by inlet temperature $(T_5 - T_0)/T_0$ against radius ratio; the design gradient of $(T_5 - T_0)/T_0$ is given by the dashed line.

Matching Rotor and Stator

The characteristic curves of adiabatic efficiency and pressure ratio against equivalent weight flow are given in figure 3 for the rotor alone. At the higher tip speeds the characteristic of this rotor is that the peak efficiency and peak pressure ratio occur at peak weight flow. This trend exists even when there is a shock in the rear of the rotor and true impulse condition is not attained. Reference 5 points out that, where recovery decreases rapidly with increasing Mach number, the optimum match point between rotor and stator may not occur at the best rotor performance point because of the rapid decrease in Mach number as the impulse condition is reached. The design or match point for the tests of stator 1 was chosen from preliminary data as $P_5/P_0 = 3.5$, $\eta_{ad} = 0.835$, $\bar{\beta}_5 = 48^{\circ}$, and $\bar{M}_5 = 1.3$. Later data and slightly different fairing as reported in reference 6 give the following data for the average flow angle of 48°: $w\sqrt{\theta}/\delta A_F = 22.3$, $P_5/P_0 = 3.5$, $\bar{M}_5 = 1.38$, and $\eta_{ad} = 0.842$. This latter point is termed the design match point for the tests of stator 1.

At lower than design rotor speeds, the choking capacity of fixed stator blades prescribes an operating line that prevents passage of the full rotor weight flow. The following equation shows that the maximum weight flow which may be passed through a given area at a fixed total pressure and temperature is a function of Mach number only:

$$\frac{w}{A p_t a_t} = \frac{w\sqrt{T}}{PA}\sqrt{\frac{R}{\gamma g}} = \frac{M}{\left(1 + \frac{\gamma-1}{2} M^2\right)^3} \quad (\text{for } \gamma = 1.4) \qquad (1)$$

(All symbols are defined in the appendix.)

For choking at the minimum area, M = 1.0, and the value of the right side of equation (1) is 0.578. The dashed line in figure 3 shows this limitation on the rotor characteristic curve for an area of $A_a \cos 48^\circ$, which corresponds to the design setting angle. Rotor weight flows above this limit line will not pass through the fixed stators even with isentropic compression from their free-stream Mach number to Mach 1.0. In any actual stator installation, some losses in pressure and build-up of boundary layer will occur between station 5 and the throat, so that a further decrease in peak weight flow is to be expected.

Stator 1

Description and design. - The first set of stators was designed for the approximate rotor-exit flow condition at 90-percent rotor design speed using an average Mach number of 1.3 and a flow angle of 48°. Later and more complete tests showed that the Mach number at the 48° angle was 1.38. In order to allow room for instrumentation, only 20 blades were used. An axial length of 5 inches resulted from a specified solidity of about 2.5. Turning of 40° was specified, and both subsonic and supersonic deceleration were to be accomplished in a single stator row. Minimum area was at the closed channel entrance (see fig. 2(a)), and the contraction ratio from a 48° streamtube was 1.014. Design blade section was determined at the mean radius using averaged rotor-discharge angle and Mach number, and the blade was untwisted; hence, there was a constant blade profile at all radii. The blade design method consisted in assuming an absolute and a tangential velocity variation along the axis, thus determining a blade mean line. Assuming isentropic flow, the variation of area necessary to fulfill these assumptions was then found. Although the mean line was based largely on experience, a rough check of blade loading was made using a linear variation of velocity across the channel according to the method of reference 7. In order to reduce the subsonic deceleration rate, an arbitrary height ratio of 1.25 was applied to the latter half of the channel in the form of a cone of about 5.5° half angle (see sketch, fig. 2(a)). From the resulting area variation a blade profile was drawn, and then a boundary-layer and loss allowance of 15 percent of the mean passage width of 2.33 inches was applied. This allowance was applied linearly with axial length, with 2/3 of the total applied to the suction surface and 1/3 to the pressure surface of the blade. Maximum allowance was at the trailing edge. A photograph of the stator is shown in figure 2(b), and blade coordinates are given in table I.

Over-all performance without cone fairing. - In order to cover a range of rotor weight flows, stator 1 was tested at three angle settings without the cone fairing and at two angle settings with the cone installed. Because of the irregular radial profiles of total pressure and energy addition at the stator entrance and the long blade length compared with height, it was impractical to present the performance on the basis of individual blade elements. Consequently, over-all results are presented here based on the integrated average of the total pressures measured by a 26-tube rake $2\frac{5}{8}$ inches downstream of the stators (station 7).

Pressure ratio: The standard characteristic map of the rotor-stator combination with stator 1 at design angle (48°) but without the cone is shown in the upper left of figure 6. At low speeds, a range of weight flow exists between open throttle and surge. Compared with the performance of the rotor alone (fig. 3), however, the operating range is reduced at both ends. The stator is unable to pass the full rotor weight flow, and stalling in the stators produces surge at higher weight flows than for the rotor alone. As operating speed is increased, the range narrows rapidly until at 75 to 80 percent of design speed the weight flow becomes virtually a unique function of tip speed. For this type of operation, at open throttle, an expansion occurs in the diverging channel, and the Mach number at the downstream measuring station frequently exceeds that at the diffuser inlet. When the proper correction for normal shock in front of the instruments is supplied, the total pressure can be determined; but this point has little value from a practical standpoint, since no diffusion has been accomplished.

As the outlet throttle is closed, back pressure increases and the normal shock is moved upstream in front of the station 7 instruments. Since the normal-shock loss is now charged to the stator pressure recovery, this recovery, and hence over-all pressure ratio, is affected by the Mach number at which the normal shock occurs. With the shock just at the stator exit, the lowest pressure ratio results (e.g., 2.23 at 80-percent speed). As the shock is forced upstream, the over-all pressure ratio increases until the maximum pressure ratio occurs at the surge point (2.45 at 80-percent speed). In all cases where no range of weight flow existed, the maximum practical pressure ratio occurred at the surge point; and, hence, the observed value of peak pressure ratio was influenced somewhat by the operator's skill at running the test rig near surge without actually entering this condition. For simplicity, other characteristic maps to be presented give only the surge point for each of the higher speeds, and it is to be understood that lower pressure ratios are available at each weight flow.

In addition to the absence of range at the higher speeds, the peak value of weight flow obtained at the stator match-point speed (90-percent rotor design speed) was 21 pounds per second per square foot of frontal area (fig. 6) compared with the design value of 22.3 and the maximum

rotor-alone value of 23.7 (fig. 3). For a fixed blade setting, if the minimum area is adequate for isentropic flow, weight flow is fixed by the losses between station 5 and the throat.

Efficiency: The adiabatic efficiency of the rotor-stator combination is given in figure 6 as a function of rotor-inlet weight flow $w\sqrt{\theta}/\delta A_F$. At low speed the efficiency peaks in a conventional manner at a value of weight flow in midrange. At higher speeds efficiency reflects the type of operation just discussed for the pressure-ratio characteristic. Peak efficiency occurs at the surge point, discounting the fictitious open-throttle points. At the stator match-point speed (90 percent) the peak adiabatic efficiency is about 0.71 at a pressure ratio of 2.83 and weight flow of 20.7 pounds per second per square foot of frontal area.

Recovery factor: The ratio of mass-averaged total-pressure ratio at station 7 to that at station 5 is plotted against average Mach number at station 5 in figure 6. This ratio, or recovery factor, is directly analogous to that of other supersonic diffusers, supersonic inlets and the like. For all rotor operating points except low-speed operation, stator-entrance Mach number is a unique function of equivalent weight flow and equivalent speed. As a result, the pressure-recovery curves exhibit the same characteristics as previously shown for pressure ratio and efficiency. In this figure the open-throttle points are of some interest. Because of the favorable pressure gradients in the diverging channel, little separation or mixing occurs. Most of the losses during this type of operation result from skin friction, mixing between the rotor and stator throat, and the external shock configuration.

Outlet Mach number: The average outlet Mach number (station 7) for stator 1 at design angle is given as a function of equivalent weight flow in figure 6. With open throttles the Mach number is beyond the top scale. As expected, outlet Mach number decreases somewhat as back pressure is applied and reaches lower values at the lower speeds.

Performance at blade angles 5° and 7.5° less than design without cone fairing. - In order to extend the range covered by the stator tests and to provide more matching information, the stator blades were reset to angles 5° and 7.5° lower than design. At a blade angle of 43° (5° below design) an improvement in weight flow was achieved at all speeds as shown at the top of figure 7, which gives only the surge points for clarity. When an additional 2.5° angle setting was made (blade angle, 40.5°), the weight flow increased at lower speeds, but little gain was evident at design speed. A comparison of pressure ratio at a given speed shows that virtually no loss in pressure ratio accompanied the gain in weight flow.

Adiabatic efficiency is plotted against equivalent weight flow for the surge points of the three angles tested in the middle section of figure 7. At the stator match-point speed (90 percent) and blade angle of

40.5°, a maximum value of adiabatic efficiency of 0.71 was reached at a pressure ratio of 2.85 and an equivalent weight flow of 22.25 pounds per second per square foot of frontal area.

The plot of recovery factor against average stator-inlet Mach number (lower part of fig. 7), shows that, for stator-inlet Mach numbers greater than 1.2, the increased blade angle of incidence actually causes more pressure loss in the stators, as might be expected. However, the increase in rotor performance gained by shifting the operating point to higher values of weight flow counterbalances the slight pressure loss due to incidence angle. This condition causes the slight change in over-all adiabatic efficiency previously noted. At the highest inlet Mach number tested (about 1.4), recovery factors were between about 0.75 and 0.80.

Performance with cone fairing on hub. - A conical fairing piece designed to reduce the stator-discharge area 20 percent was tested at the 48° and 43° blade settings to allow comparison with the straight-hub data. The characteristic map for these tests is given in figure 8 (surge points only). As compared with the tests without the cone at design angle and 90-percent speed, weight flow increased insignificantly to 21.15 pounds per second, but the design value of 22.3 was not reached. There was virtually no change in pressure ratio or efficiency due to installation of the cone. However, at the 5° lower blade setting the pressure ratio was slightly higher and weight flow unchanged, compared with the straight-hub case. At 90-percent speed, pressure ratio was 2.91 at a weight flow of 22.35 pounds per second per square foot of frontal area.

The adiabatic-efficiency plot shows about a 1-percent improvement at the 43° blade angle (0.72) compared with that at the design angle. Comparison with the corresponding straight-hub tests shows only a slight change attributable to the cone fairing, virtually within the margin of accuracy of the tests.

At design angle, the curve of recovery factor against Mach number in figure 8 is almost identical with that for the straight hub. At 43° blade angle, the recovery factor improves somewhat in the lower Mach number range.

A comparison at 90-percent speed between the design angle with straight hub and the 43° blade angle with cone fairing shows 1-percent gain in adiabatic efficiency. The gain in efficiency stems from the improved rotor-stator matching, inasmuch as a loss in stator recovery factor of 3 percent exists. To summarize the results of the tests of stator 1 at 43° blade angle with cone fairing, at 90-percent speed a pressure ratio of 2.91 was attained at an efficiency about 0.72 with a weight flow per unit frontal area of 22.35 pounds per second per square foot. Average Mach number at the stator-exit measuring station was 0.67, and average outlet flow angle was 7°.

Static pressures at 90-percent speed. - Design angle, without cone fairing: The pressures from static taps on the blades and on the outer wall allow an insight into the behavior of flow in the channel and will be discussed for operation at 90-percent speed with and without cone fairing. At the peak-efficiency weight flow of 20.7 pounds per second per square foot frontal area for stator 1 without cone fairing (fig. 6), the average rotor-exit conditions are Mach number of 1.24 and flow angle of 49°.

The ratios of static pressure to inlet tank pressure for taps on the blade and outer wall for the open-throttle condition (fig. 9(a)) indicate that, after some expansion waves on the suction surface and several weak oblique shocks on the pressure surface, the air expands supersonically as the area increases, resulting in an average Mach number of 1.8 at the downstream measuring station. Despite the favorable pressure gradient on all surfaces over most of the axial length, the recovery factor was only 0.90 (fig. 6), indicating considerable loss due to mixing in the region before the throat and friction on walls and blades.

As back pressure is applied by throttling downstream, a normal-shock wave is forced upstream and flow at the measuring station is subsonic. This wave, which is shown at about midchord (fig. 9(a) for "increased back pressure"), appears as a sharp rise in static pressure. Pressures upstream of this wave are unaffected by it and agree well with those observed with the open-throttle condition. Inasmuch as the pressure loss through this shock is now charged to the stators, the recovery factor is only 0.777 and Mach number at the measuring station is now 0.671 (fig. 6).

Further application of back pressure moves the shock upstream, as shown in figure 9(a) for "more back pressure." For this condition, recovery factor is 0.83 and outlet Mach number is 0.55 (fig. 6).

At the surge point (fig. 9(a)), there is no sharp pressure rise on the pressure surface, indicating that the shock wave has merged with the external waves into a single shock configuration ahead of the first static tap. From the location of the pressure rise on the outer wall and on the suction surface, an approximate wave may be drawn in as shown by the dotted line. Recovery factor for this test point was 0.856, and average outlet Mach number was 0.555 (fig. 6).

Pressures at the first two stations on the suction surface and the three outer-wall taps in the plane of the leading edge remain unaffected by the application of back pressure. The decrease in recovery factor from 0.90 for open throttle to 0.856 for the surge point reflects the loss through the normal shock as well as additional subsonic losses resulting from separation, mixing, and other viscous effects. Similar pressure plots have been made for operation at 5° and 7.5° lower setting angles without the cone fairing. In general, these plots are very similar in nature and exhibit no major changes due to setting angle.

With cone fairing: Figure 9(b) shows the 90-percent-speed surge point at design angle with the cone fairing, which compares directly with figure 9(a) for the condition at surge without cone fairing. The surge plots are very similar except for slightly greater acceleration along the suction surface before the normal shock with the cone. There is no evidence of increased velocity in the rear half of the blade passage as might be expected from the reduction in area. It appears that the excess area previously occupied by the separated flow adjusts to the presence of the cone and that the cone size is insufficient.

The corresponding plot for the 43° blade angle at 90-percent speed with the cone installed is given in figure 9(c). This test point is included because it proved to be the best operating point for the rotor-stator combination, even though the recovery factor of 0.827 is slightly lower than for the design angle setting (fig. 8). Again, the subsonic diffusion is very similar to previous conditions, and there is a slight change in the position of the normal shock.

The over-all static-pressure ratio on the suction surface is about 2.1. Of this over-all ratio, the greater part, about 1.6, appears to be due to the normal shock. Tables of normal-shock relations give a Mach number of 1.23 for this static-pressure ratio of 1.6 and a total-pressure recovery of 0.9896 at Mach 1.23. The free-stream inlet relative Mach number is 1.295 where pressure recovery is 0.9802.

From these values, it is evident that the greater part of the losses through these blades is not due to the normal shock. Instead, the friction and mixing before the normal shock and the separation, secondary flow, and mixing behind it (which may be aggravated by it) constitute the major sources of loss.

Recovery-factor profiles. - In order to get additional information on the loss phenomena in the stator passages, the estimated recovery factor in the circumferential direction was determined by dividing the 26-tube-rake readings at several radial positions by the total pressure at corresponding radii at the stator entrance. Because the flow streamlines do not remain at the same radius through the stator passage, and because of the nonuniform inlet total-pressure profile, it was sometimes possible to compute recovery factors over 1.0 by this method. However, when plotted as profiles of constant recovery factor, these calculations give a qualitative picture of the secondary flows and loss regions occurring in the blade passages.

Figure 10(a) shows such a plot for open-throttle operation at 90-percent speed for 43° blade angle without the cone fairing. The circumferential distance of this plot represents the spacing between two blades; but the blade wakes are not necessarily at the extremities of the plot because of the fixed rake location and the variable flow angle. In fact,

in this particular plot, the blade wake is quite clearly at 0.5 inch circumferential distance. In the corners formed by the suction surface and the walls, two large cores of low-energy air may be seen that are typical of passages with large secondary flows. In the middle of the passage, the recovery factor is high over a large region, indicating that the external shock configuration was not strong. Average outlet Mach number was 1.353. The average recovery factor for this test point, obtained by arithmetically averaging the 26 tubes circumferentially and mass-weighting the averages radially, was 0.835. By mass-weighting each point, both radially and circumferentially, a recovery factor of 0.869 was obtained. Since all recovery factors reported herein were obtained by the former method for simplicity, they are considered conservative.

The recovery profile for the surge-point flow for the same blade configuration and rotor speed is given in figure 10(b). It is apparent that more mixing takes place and that the spread between high and low recovery factor is reduced a great deal. The same core of high recovery factor exists, although peak values are lower and the area covered by high recovery has decreased. The two regions of lower-energy air are larger but do not have the extremely low recovery of the open-throttle condition. Average recovery factor at this condition was 0.817 (0.831 by double-mass-weighting), and the average discharge Mach number was 0.549.

Similar profiles are given in figures 10(c) and (d) for the design-angle and the 40.5°-angle surge points. In both cases, flow is very similar and there is no apparent change that can be ascribed to the changed angle settings. In addition, the profiles for the two angle settings with the cone installed are given in figures 10(e) and (f). There is no large effect at station 7 due to the presence of the cone, and the two loss vortices have about equal area and recovery level.

Mach number profile. - The Mach number profile is given in figure 11 for the surge point at 90-percent speed and at design angle setting without cone fairing. This profile appears quite different from its counterpart for recovery factor (fig. 10(c)). There are two main regions: (1) the high-velocity region, which is coincident with the high-recovery-factor region, and (2) a low-velocity region, which covers the area of the secondary flow and low-energy air. There is no evidence of the two separate loss cores shown by the recovery-factor profile. The large gradients in Mach number at this measuring station indicate that further mixing losses would be sustained downstream.

Stator 2

Description and design. - Stator 2 was intended as a refinement of stator 1 in which an effort was made to match the angles and Mach numbers in the radial direction at the stator entrance. For this blade, three

elements - hub, tip, and mean radius - were designed individually and then stacked to match inlet angles. Inlet conditions were $M = 1.35$ and $\beta = 53^\circ$ for the tip, $M = 1.37$ and $\beta = 45^\circ$ for the mean radius, and $M = 1.4$ and $\beta = 43^\circ$ for the hub. An incidence angle of 5° was specified at all radii, so that design blade angle at the mean radius was 40°. All sections turned to 8° and decelerated to $M = 0.7$. No contraction was prescribed between streamtube and throat section. At the tip and hub the throat occurred at the closed channel entrance; but, because of application of the boundary-layer allowance, the throat at the pitch section was at the station 1.8 inches from the leading edge. Cone fairing of height ratio 1.25 was used, and boundary allowance of 15-percent passage width was applied 2/3 to suction surface and 1/3 to pressure surface as for stator 1. These blades were laid out and machined in a flat plane and then turned to fit the helical flow path. As a result, some of the tip element was cut away, resulting in less twist than design. A photograph of these stator blades at a blade setting 3° higher than design is given in figure 12. At the pitch radius, this blade angle of 43° corresponds exactly to stator 1 at the second angle setting.

Over-all performance. - The second stator design was tested at three blade angle settings, 40°, 35°, and 43°, with cone fairing installed at all three settings. The operation of these stators was very similar to that of stator 1, in that there was a limited operating range at low speeds and a vertical operating line at the higher speeds. For clarity, however, only the surge points are included in the characteristic map in figure 13. Comparison of the design setting of 40° with the 40.5° setting of the first stator (fig. 7) shows virtually the same weight flow at all speeds and a slight decrease in pressure ratio at the higher speeds. (Cone fairing was used only with stator 2.)

Resetting the blades at a 5° lower angle did not accomplish as much increase in weight flow as similarly resetting the blades of stator 1 (fig. 8), indicating that the initial setting angle was closer to the limiting incidence angle. An additional blade setting 3° in the opposite direction caused a slight drop in weight flow accompanied by an increase in pressure ratio. At the pitch radius this 43° blade setting for stator 2 is comparable to stator 1 at 5° less than design. A comparison of figures 7 and 13 shows both blades to be on the same operating line. However, at each speed, stator 2 operates at a slightly lower weight flow and over-all pressure ratio than stator 1. An increase in losses before the throat could produce such an effect, reducing the weight flow and the over-all recovery. The improved angle matching at the stator entrance should have resulted in an opposite effect.

Figure 13 also shows a plot of adiabatic efficiency against equivalent weight flow for the three angle settings. At low speeds, the design angle setting is slightly more efficient, but otherwise the three configurations are much the same. Compared with stator 1 at design angle (fig. 7), this

twisted-leading-edge blade had about the same over-all efficiency. However, stator 1 at 43° angle had better performance at all tip speeds.

Stator 2 recovery factor is plotted against inlet relative Mach number for the three settings in the lower part of figure 13. At 90-percent speed the data were inconsistent, and as a result a single curve has been faired through the points. Comparison with the equivalent curve for stator 1 (fig. 7) shows no improvement at any Mach number and slightly lower values of recovery over most of the range. As a whole, the performance of stator 2 was disappointing, in that it showed no clear superiority to the first stator tested.

Static pressures. - Pressures along the flow path and on the blade surfaces of stator 2 are given in figure 14(a) for the 70-percent-speed surge point with the blade angle of 43°. A recovery factor of 0.891 was attained at an inlet Mach number of 1.02 (fig. 13). Estimates of maximum and minimum Mach numbers are given based on total pressures in front of and behind the stators. At the stator outlet the circumferential average total pressure was used. The indicated maximum and minimum Mach numbers on the blades show that the flow is entirely subsonic except for the immediate vicinity of the leading edge on the suction surface. The position of the shock wave is apparently forward of the throat of the blade passage, which for this blade is well inside the channel. In the front part of the blade channel, there is some acceleration of the flow due to area contraction, and a gradual deceleration takes place in the rear. Average exit Mach number was 0.621.

At the surge point at 90-percent speed, the pressures and estimated Mach numbers in figure 14(b) were observed. There was evidently an acceleration around the leading edge, followed by a region of fairly uniform pressure. The normal-shock wave was in the center of the channel formed by two blades at approximately the position of the start of the wedge fairing. Recovery factor was 0.828 at the inlet relative Mach number of 1.295 (fig. 13), compared with the recovery factor of 0.835 with the untwisted stator blade. Thus, there was no improvement in the over-all pressure recovery due to the improved angle matching of this stator. A comparison of the pressures on this blade with those on stator 1 at 43° blade angle (fig. 9(c)) shows considerable difference in the region from the leading edge to the throat. With the first blade, it was possible to stabilize the shock farther forward without surging the compressor. There was also less expansion along the suction surface, which resulted in a decrease in the amount of deceleration necessary. With slight changes in thickness of the twisted stator, it might be possible to improve the performance.

Recovery-factor profiles. - Numerous profiles of constant recovery factor similar to those presented for stator 1 were made for the second stator. In general, these plots are very similar to those of the first

stator, in that they show the large amount of viscous effects common to the low aspect ratio and high solidity. The recovery-factor profile for the 43° blade angle at the 90-percent-speed surge point is shown in figure 15. As in the first stators, the high-recovery core is surrounded by low-energy regions that occupy the greater part of the passage. At this condition, average inlet relative Mach number was 1.295, average outlet Mach number was 0.666, and average recovery factor was 0.828.

Stator 3

Description and design. - Stator 3 was an untwisted double-circular-arc airfoil with a camber angle of 52°, chord length of 3.2 inches, and maximum thickness of 7 percent of chord. The leading- and trailing-edge radii were 0.02 inch. These blades were the same as those used with the transonic rotor of reference 8 and were shortened to fit the passage height behind this rotor with the cone fairing moved forward. The solidity for 20 blades was 1.37, compared with approximately 2.5 for stators 1 and 2. The aspect ratio was 0.35 compared with 0.19 for stators 1 and 2. The purpose of the investigations with this stator was (1) to extend the range of Mach number covered for this airfoil, and (2) to determine the effect of lowering solidity and increasing aspect ratio. The initial setting was made for a 5° incidence angle, which meant the angle of the camber line was 43° at the leading edge and -9° at the trailing edge. Minimum area in the channel occurred at the "closure point" normal to the pressure surface at the leading edge. Throat area was greater than streamtube area at either 48° or 43° flow angle.

Six static taps were installed on the pressure surface and six on the suction surface of the blades at 1/2-inch axial spacing. The original intent of these tests was to extend the range of Mach number coverage for this type of airfoil, since the tests for the transonic rotor did not go above 0.76 inlet Mach number relative to the stators. Even at 50-percent rotor speed, the outlet Mach number of this rotor was 0.74. Thus, there was very little overlapping of the Mach number range. Because of the poor performance of these blades and the changes in solidity and aspect ratio, direct comparisons with reference 8 could not be made. (Flow separated from the suction surface at most operating points.)

Over-all performance. - The standard characteristic map for the initial setting of the double-circular-arc blades at 43° blade angle is shown at the top of figure 16. At 90-percent speed, this set of stators passed slightly more weight flow than the first set at 48° blade angle (fig. 6) but less than the same blades at the 5° lower setting (fig. 7). Compared with the original design match point for the stators (22.3 (lb/sec)/sq ft), weight flow is 2 percent low, even though available throat area is greater than streamtube area. At all speeds, some slight range of weight flow is evident, narrowing to 1/2 pound per second at

design speed. There appears to be a discontinuity in the surge line at 90-percent speed that may have resulted from the indefinite nature of the surge point with this blade configuration. The violence of the surge pulsation was much lower for this stator than for stators 1 and 2.

Curves of adiabatic efficiency against weight flow are also given in figure 16. At the higher speeds, over-all pressure ratio is lower than for stators 1 and 2, and as a result efficiency decreases rapidly with increasing speed and weight flow and is generally lower than for blades 1 and 2. At all speeds the peak efficiency occurs at weight flows above the surge value.

The plot of recovery factor against stator-inlet relative Mach number in figure 16 shows that, as Mach number is increased, recovery factor decreases more rapidly than for stators 1 and 2 and reaches the very low surge-point value of 0.675 at a Mach number of 1.4. The normal-shock recovery factor at this Mach number is 0.958. Open-throttle recovery was also low, thus indicating large shock losses.

Performance at blade angle of 38°. - To extend the weight-flow range covered by these stator tests and to allow better matching with the rotor performance, the blade angle was reset 5° lower at 38°. The performance of this configuration, which was determined at the surge points only, is given by solid data points in figure 16. At all speeds, it is evident that there was no large improvement in over-all performance as a result of the angle change. At low speeds, a slight improvement in recovery factor resulted in slight improvement in adiabatic efficiency; while at higher speeds, the reverse was true. At the 90-percent-speed surge-point weight flow of 20.21 pounds per second per square foot, the stator-inlet flow angle is 50.5°. The resulting incidence angle of 12.5° is considered excessive for the Mach number range.

Static pressures. - The static-pressure measurements on the blade surfaces and on the outer wall of stator 3 are given as ratios to the inlet tank pressure for the surge point at 50-percent speed in figure 17(a). Average inlet relative Mach number was 0.75 (fig. 16), and average outlet Mach number was 0.464. Estimates of the maximum and average minimum Mach numbers are also given based on average total pressures in front of and behind the stators. On the suction surface immediately behind the leading edge, a local expansion reduces the static pressure and increases the Mach number to values much higher than the stream value. Beyond this point, there is a rapid compression followed by a more gradual pressure rise. The pressure changes very little all along the blade pressure surface, indicating that a rise from the stream value occurs before the first static tap (an external shock configuration). All Mach numbers behind this shock are subsonic and decrease gradually up to the last inch, where the mean line turns past the axial direction. With the height of the cone fairing still increasing at this point, the net flow area decreases, thus accounting for the slight acceleration.

As tip speed and inlet relative Mach number are increased, the pressure gradients become more severe, as shown in figure 17(b) for the surge point at 70-percent speed. Inlet Mach number was 1.0 for this point (fig. 16). Again, the first measurement on the suction surface indicates much higher Mach numbers than the free-stream value, showing the acceleration around the leading edge. This high velocity exists only on the suction surface; the Mach number is much lower in the passage, and on the pressure surface Mach numbers are quite low. It seems probable that the steep pressure gradients on the suction surface give rise to separation of the flow, resulting in a great deal of mixing and pressure loss. These minimum Mach numbers on the suction surface may be smaller than those shown, because total pressure in the separated region is less than average. On the pressure surface the gradients are much smaller, and separation is not expected. Average inlet flow angle was about 50°, resulting in 7° incidence angle at mean radius.

Much the same picture is presented by the surge point at 90-percent speed (fig. 17(c)), except that the gradients are still more severe. The behavior of this blade illustrates an important limitation of circular-arc blades at high stagger angles for flow with supersonic entrance Mach number. The high rate of curvature of the blade near the leading edge initiates an expansion wave that accelerates the flow on the suction surface before the presence of the pressure surface is felt. On the other hand, the rounded leading edge and blade curvature are probably responsible for the range of weight flow, limited though it is.

Recovery-factor profiles. - Profiles of constant recovery factor are given in figure 18 for the three speeds just discussed. At 50-percent speed, where inlet relative Mach number is 0.75, there is a large region of high recovery very near a region of much lower recovery (fig. 18(a)). There is no evidence of the double loss cores and the secondary-flow phenomenon as for stator 1 (fig. 10). However, it is clear that flow is separated from the suction surface and that most of the flow issues from the blades as a jet. Average outlet Mach number is 0.464.

At 70-percent speed (fig. 18(b)), inlet Mach number is 1.0 and recovery profiles are similar to those for the 50-percent speed. Again, the wake appears to be along a radial line, and there is a large single low-energy region. At 90-percent speed (fig. 18(c)), inlet Mach number is 1.20, and some changes are evident compared with the lower speeds. The entire recovery level is lower than for 50-percent speed, the low-recovery region is shifted toward the outside wall, and the higher-recovery region is shifted inward.

However, even at this low average recovery of 0.742, there is no evidence of the double-core type of secondary-flow phenomenon shown for stators 1 and 2 (figs. 10 and 15). This fact is due, in some measure at least, to the higher aspect ratio and lower solidity of these blades.

The loading on these blades was excessive because of the high camber angle. Blades of double-circular-arc section, designed expressly for the stator-entrance condition specified by this rotor, would probably be thinner and have less camber angle if contemporary loading restrictions were to be observed. However, the expansion around the leading edge on the suction surface would still result in high Mach numbers at the first shock wave.

The Mach number profiles for stator 3 are given in figure 19 for the surge point at 70- and 90-percent speed. In general, these plots show the same characteristics exhibited by the recovery profiles but emphasize the large difference in velocity level between the high- and low-recovery regions. Additional losses due to mixing would thus be anticipated. In large areas of the passage width, there is very little flow, indicating a large separation region, presumably off the suction side of the blade.

Losses in Annulus without Stators

The results of the tests with three different sets of stators show unexpectedly high losses even with low subsonic inlet relative Mach numbers. For instance, the original double-circular-arc stators (stator 3 herein and reported in ref. 8) had an indicated recovery factor of 0.968 at an inlet relative Mach number of 0.76. As installed behind this supersonic rotor, however, the recovery factor was only 0.933 at an inlet relative Mach number of 0.75. It should be noted that the span of the blade was cut in half so that end effects would be relatively more important.

Annulus recovery factor. - The mass-weighted average pressure ratios at stations 5 and 7 have been placed in the form of an "annulus recovery factor" for a number of test points obtained during rotor performance tests without stators. These data are given in figure 20 to the same scale as for the stator recovery factor. The scatter of test points may result from the fact that the flow-path length varies with flow angle at a given Mach number. The figure shows that there is a trend of increasing loss with increasing Mach number. In addition, it is apparent that substantial pressure loss exists between stations 5 and 7 even at relatively low Mach numbers. This indicated loss is due not only to friction and mixing, but possibly also to erroneous measurement at station 5. The flow at station 5 is fluctuating because of blade wakes and rotor channel secondary flows, which cause both temperature and pressure measurements to read above a true average. If the average loss shown by this figure were deducted from the losses displayed by the various stator configurations, the stator performance shown previously would seem more reasonable. Of course, this act would not improve this rotor-stator combination, but it might indicate the stator potentialities with a better rotor.

Distribution of losses. - The distribution of losses will be examined for stator 1 operating at 90-percent speed at design angle without cone fairing. From figure 3, at the maximum weight flow of 21 pounds per second the station 5 pressure ratio was 3.35. Figure 20 shows an annulus recovery factor of 0.92 at the corresponding Mach number of 1.25. Thus, station 7 pressure ratio without stators was 3.08. The open-throttle recovery factor for stator 1 (fig. 6) shows a value of 0.90 or a loss of 10 points. Thus, the additional losses due to friction on the blade surface and the shock losses at the leading edge amount to an additional 2 points compared with 8 points for the annulus alone. At the surge point where the second shock has been stabilized in front of the stator, most of the passage has subsonic flow and the recovery factor is 0.856. Static pressures on the blade (fig. 9(a) for open throttle) indicate that the normal shock takes place at a Mach number of 1.2 where the recovery factor is 0.993. Thus, very little loss can be attributed directly to the normal shock. Of the 5-point difference between the open-throttle and surge-point recovery factors, 4 points must be attributed to viscous effects. As shown by the profiles of figure 10(c), two large regions of low-energy air developed, and additional mixing losses can be expected.

If these extremely qualitative figures were to be taken literally, then, the total loss of 15 points could be divided as follows: 55-percent normal annulus mixing and wall friction loss and instrument difference, 16-percent shock and stator blade friction loss, and 29-percent subsonic viscous loss. Even if these percentages are off by 100 percent, it is still evident that the Mach number effect is not solely due to shock losses. Reference 9 points out that the mixing losses resulting from a nonuniform Mach number gradient increase rapidly with increasing Mach number.

It seems evident that good stator performance depends greatly on the type of flow received from the compressor rotor and the condition of the wall boundary layers at the stator entrance. If possible, the stator entrance should receive flow with uniform Mach number, flow angle, and energy level. In addition, the wetted area should be kept as low as possible to minimize skin friction.

SUMMARY OF RESULTS AND CONCLUSIONS

The following results were obtained from an investigation of three different sets of stators installed in a supersonic compressor:

1. With the first stator at a 43° blade angle and with cone fairing on the hub, a pressure ratio of 2.91 was obtained at an efficiency of 0.72 and an equivalent weight flow of 22.35 pounds per second per square foot of frontal area at an equivalent tip speed of 1260 feet per second (stator match-point design speed).

2. At speeds higher than 980 feet per second (70 percent of rotor design speed) there was no operating range of weight flow for stators 1 and 2, although weight flow could be changed by changing the stator blade angle.

3. The pressure recovery for the first two stators was unexpectedly low at subsonic Mach numbers and decreased to values varying from 0.75 to 0.80 at an inlet Mach number of 1.4.

4. Neither changing the subsonic deceleration rate by use of a cone fairing nor matching inlet flow angles effected any significant improvement in the performance of the particular blade configurations tested.

5. The double-circular-arc type of stator blades (third stator tested), with lower solidity and rounded leading edges, had some range of operation, though narrow, at all tip speeds.

6. Because of the expansion on the suction surface of this third stator, Mach numbers before the normal shock were high, resulting in large shock losses and separation of the flow. Recovery factors decreased rapidly with increasing Mach number; and, at an inlet Mach number of 1.4, pressure recovery was only 0.675 at 90-percent speed.

7. A breakdown of the losses at the design operating point for the first stator shows that normal-shock losses represented only about 16 percent of the total loss. Viscous effects between the rotor and stator throat and after the normal shock (plus possible instrument errors) accounted for the other 84 percent of the loss. Fifty-five percent of the total losses were observed in the annulus without stators; consequently, only about 29 percent of the loss could be ascribed to separation in the stators resulting from shock - boundary-layer interaction.

At inlet relative Mach numbers below 1.4, when curvature of the suction surface is kept small, the main losses occur as a result of secondary flows and the mixing of nonuniform gradients of Mach number and energy that come from the rotor. Thus, improvements in rotor-discharge conditions are necessary for improvements in the performance of the stators. Good over-all rotor performance is only part of the requirements for good stage efficiency. Nearly uniform stator-entrance conditions with small end-region boundary layers are desirable. It may be necessary to remove wall boundary layers in front of supersonic stators, and perhaps even the boundary layers on the blade itself.

Secondary flows may be reduced by increasing aspect ratio and decreasing solidity. For a prescribed turning, fairly high solidity may be necessary, however, to keep loading parameters low.

Because of the extreme circumferential variation in pressures and temperatures behind stators, instrumentation that is movable in the circumferential direction would help greatly in establishing loss profiles.

Lewis Flight Propulsion Laboratory
National Advisory Committee for Aeronautics
Cleveland, Ohio, June 28, 1955

APPENDIX - SYMBOLS

A	area, sq ft
a	sonic velocity, ft/sec
g	acceleration due to gravity, 32.174 ft/sec^2
M	Mach number
$\overline{M}$	mass-weighted average Mach number
P	total pressure, lb/sq ft
R	gas constant, 53.3 ft-lb/(lb)($^\circ$R)
T	total temperature, $^\circ$R
w	weight flow, lb/sec
β	flow angle, deg
γ	ratio of specific heats
δ	ratio of inlet total pressure to NACA standard sea-level pressure of 2116 lb/sq ft
η_{ad}	adiabatic temperature-rise efficiency
θ	ratio of inlet total temperature to NACA standard sea-level temperature of 518.7° R
ρ	density, lb/cu ft

Subscripts:

a	annulus
F	frontal
t	stagnation conditions
0	inlet tank
2	after guide vanes
5	after rotor

7 after stator

Superscript:

$\bar{}$ (bar) mass-weighted average value

REFERENCES

1. Ferri, Antonio: Preliminary Analysis of Axial-Flow Compressors Having Supersonic Velocity at the Entrance of the Stator. NACA RM L9G06, 1949.

2. Klapproth, John F., Ullman, Guy N., and Tysl, Edward R.: Performance of an Impulse-Type Supersonic Compressor with Stators. NACA RM E52B22, 1952.

3. Jacklitch, John J., Jr., and Hartmann, Melvin J.: Investigation of 16-Inch Impulse-Type Supersonic Compressor Rotor with Turning Past Axial Direction. NACA RM E53D13, 1953.

4. Tysl, Edward R., Klapproth, John F., and Hartmann, Melvin J.: Investigation of a Supersonic-Compressor Rotor with Turning to Axial Direction. I - Rotor Design and Performance. NACA RM E53F23, 1953.

5. Hartmann, Melvin J., and Tysl, Edward R.: Investigation of a Supersonic-Compressor Rotor with Turning to Axial Direction. II - Rotor Component Off-Design and Stage Performance. NACA RM E53L24, 1954.

6. Wilcox, Ward W.: Investigation of Impulse-Type Supersonic Compressor with Hub-Tip Ratio of 0.6 and Turning to Axial Direction. I - Performance of Rotor Alone. NACA RM E54B25, 1954.

7. Stanitz, John D.: Approximate Design Method for High-Solidity Blade Elements in Compressors and Turbines. NACA TN 2408, 1951.

8. Sandercock, Donald M., Lieblein, Seymour, and Schwenk, Francis C.: Experimental Investigation of an Axial-Flow Compressor Inlet Stage Operating at Transonic Relative Inlet Mach Numbers. IV - Stage and Blade-Row Performance of Stage with Axial-Discharge Stators. NACA RM E54C26, 1954.

9. Stewart, Warner L.: Investigation of Compressible Flow Mixing Losses Obtained Downstream of a Blade Row. NACA RM E54I20, 1954.

TABLE I. - BLADE COORDINATES FOR STATOR 1

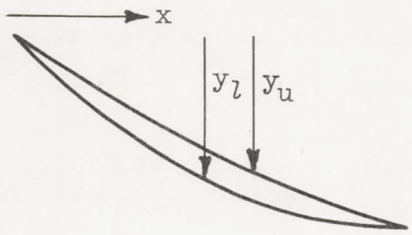

x, in.	y_l, in.	y_u, in.
0	0	0
.25	.30	.25
.50	.60	.475
.75	.88	.685
1.00	1.14	.89
1.25	1.39	1.08
1.50	1.61	1.26
1.75	1.83	1.42
2.00	2.03	1.575
2.25	2.20	1.72
2.50	2.34	1.86
2.75	2.47	2.00
3.00	2.58	2.12
3.25	2.67	2.24
3.50	2.75	2.35
3.75	2.81	2.46
4.00	2.85	2.56
4.25	2.88	2.65
4.50	2.89	2.735
4.75	2.80	2.82
5.00	2.90	2.90

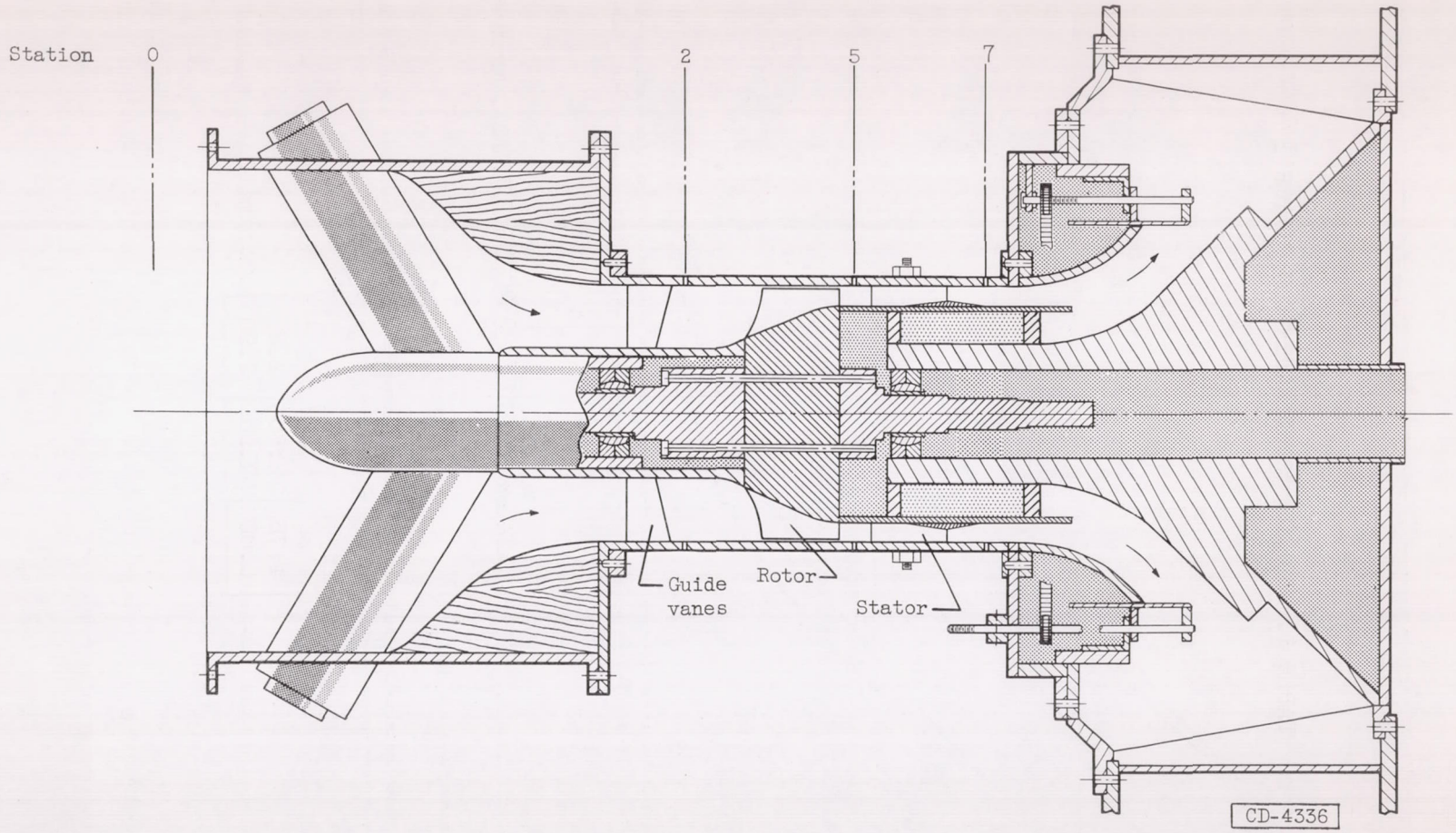

Figure 1. - Schematic sketch of rotor and stator installed in variable-component test rig.

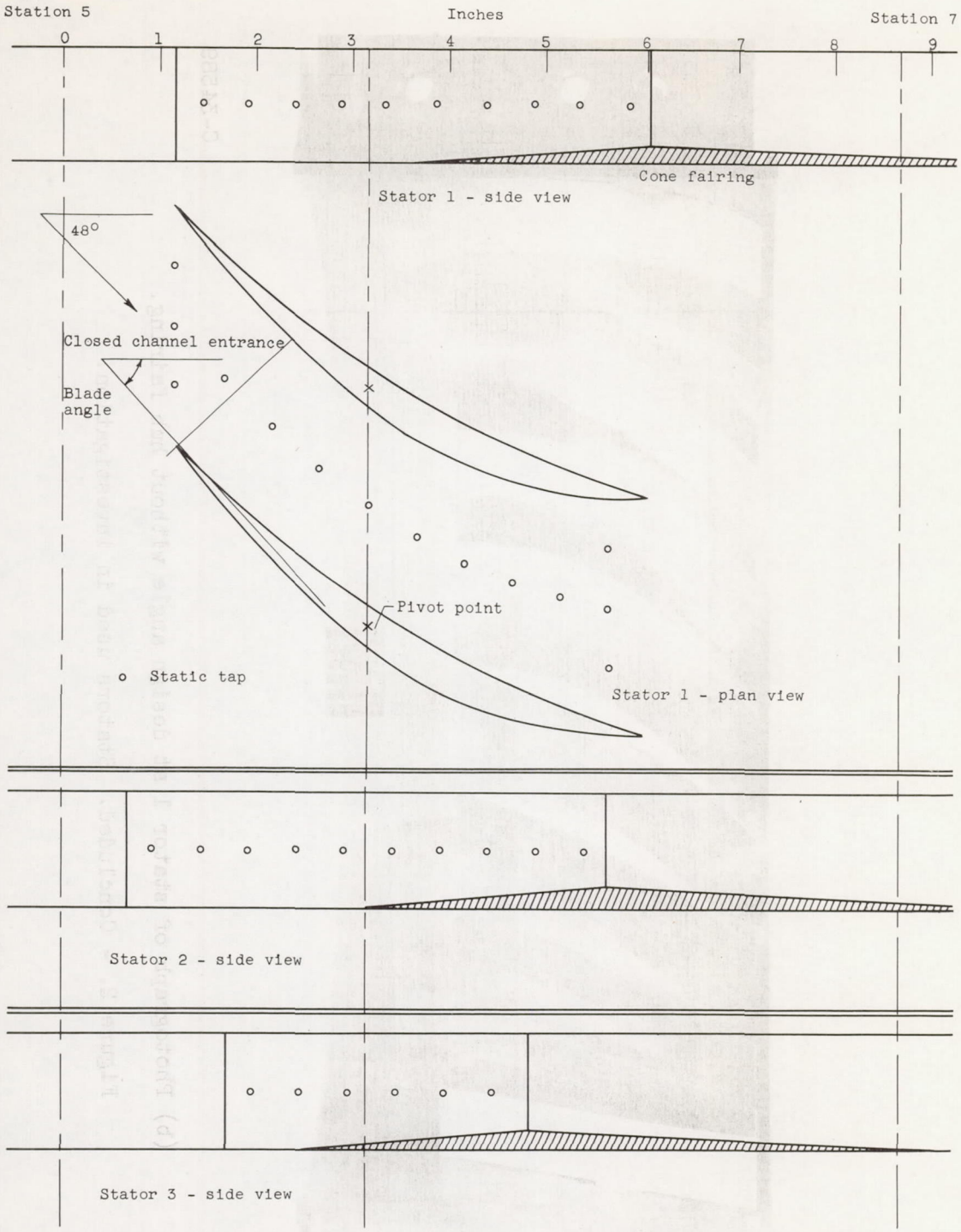

(a) Sketches showing location of static taps, cone fairing, and measuring stations.

Figure 2. - Stators used in investigation.

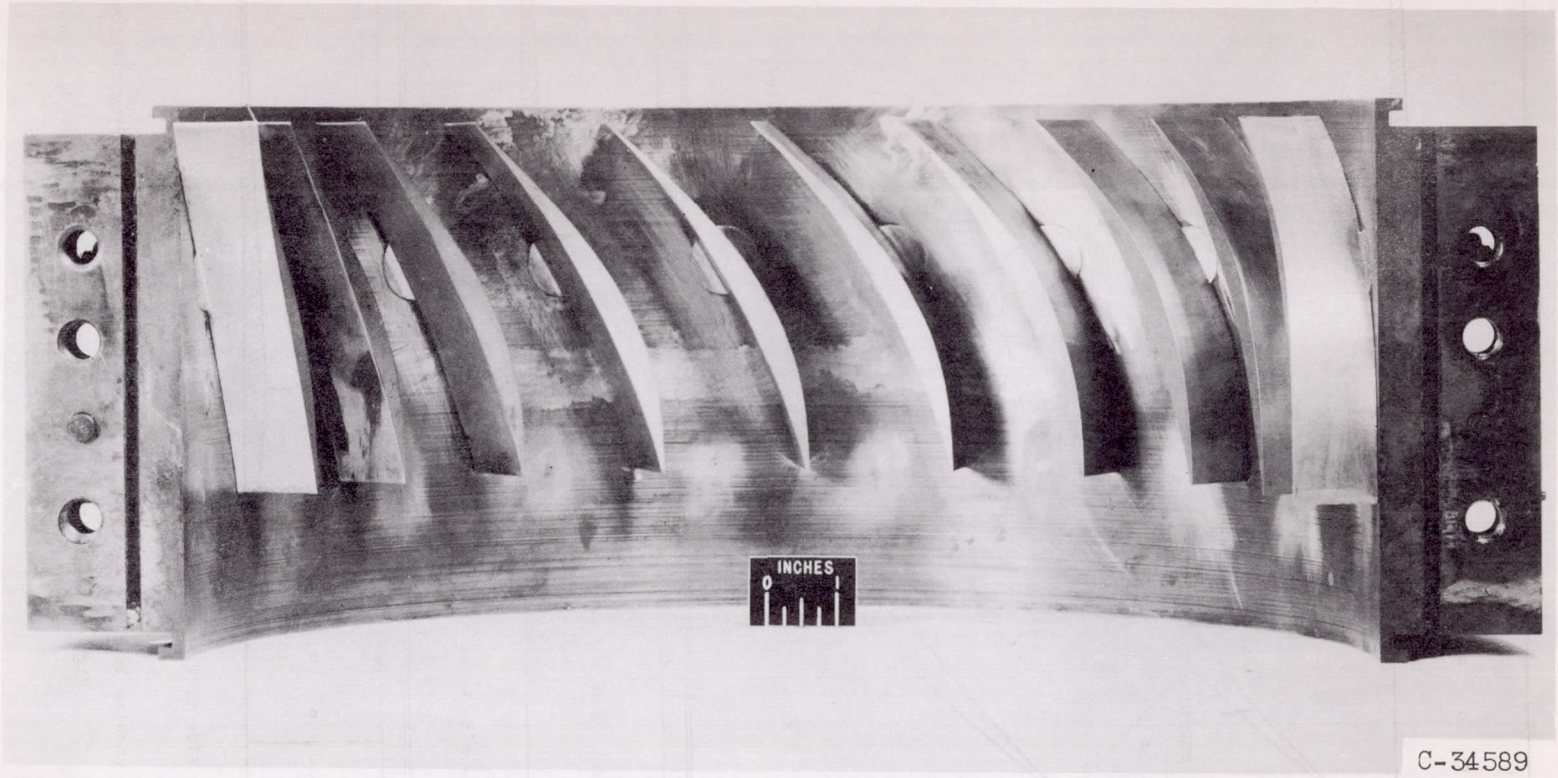

(b) Photograph of stator 1 at design angle without hub fairing.

Figure 2. - Concluded. Stators used in investigation.

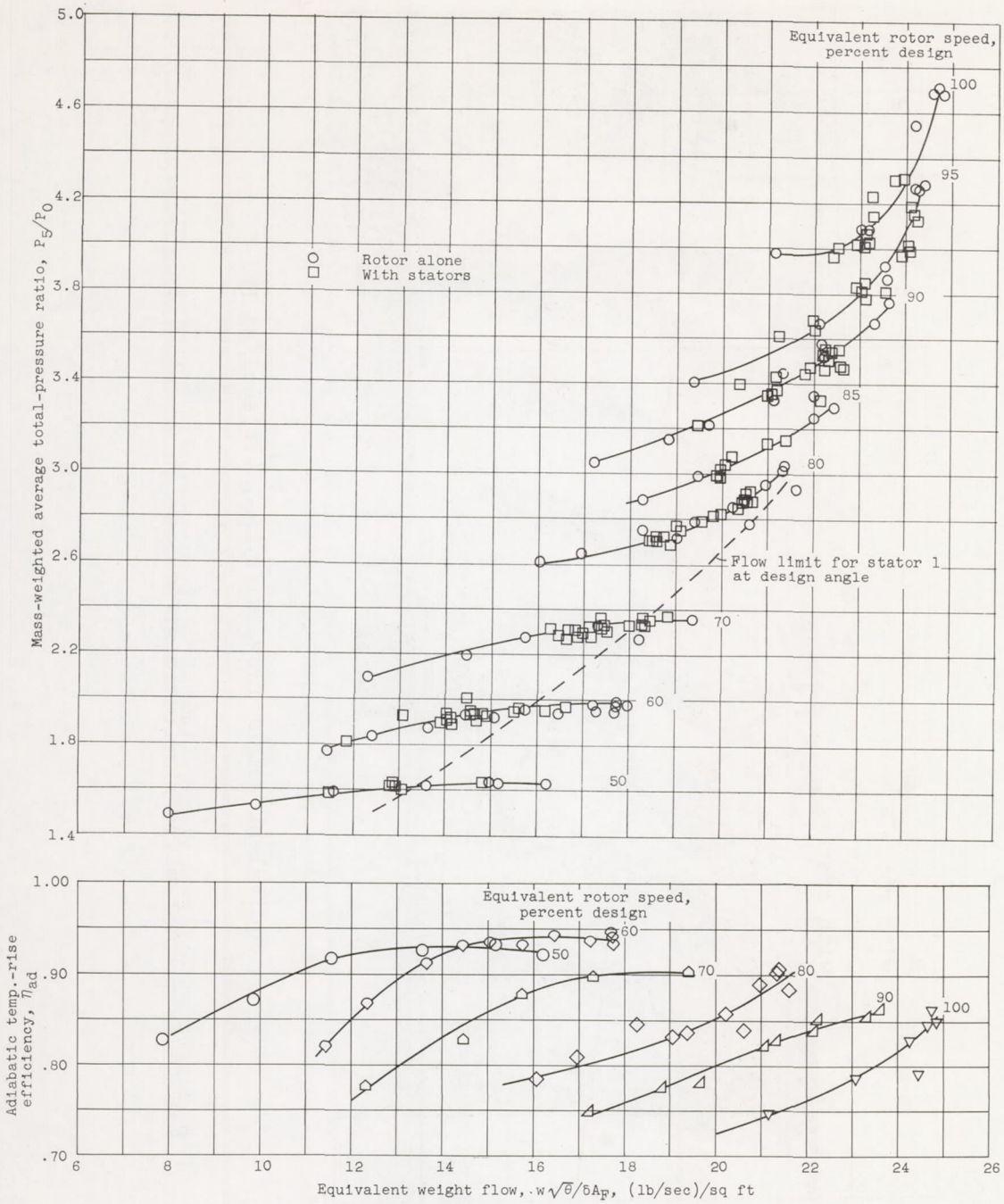

Figure 3. - Rotor characteristic curves.

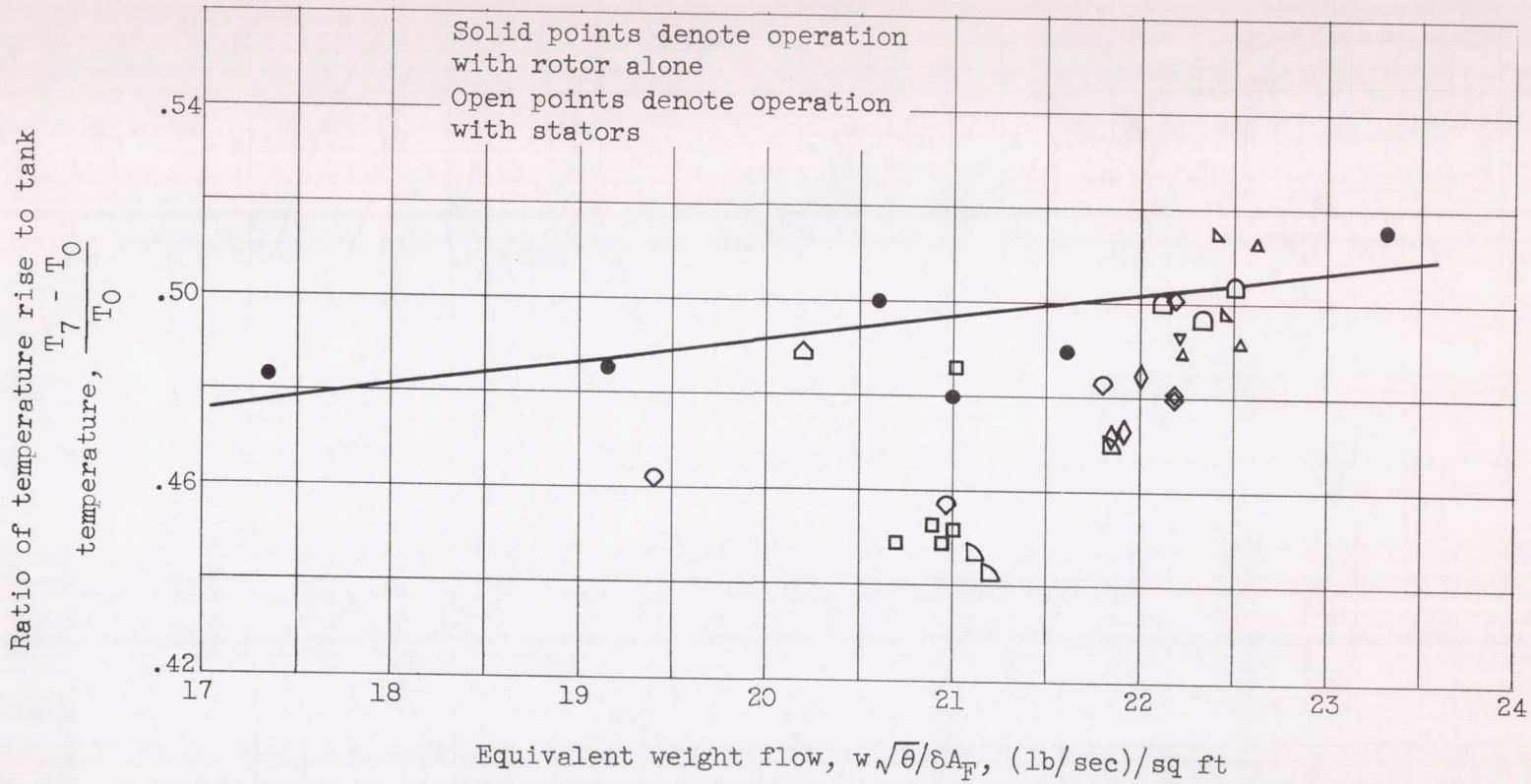

Figure 4. - Temperature-rise ratio at 90-percent design speed (station 7).

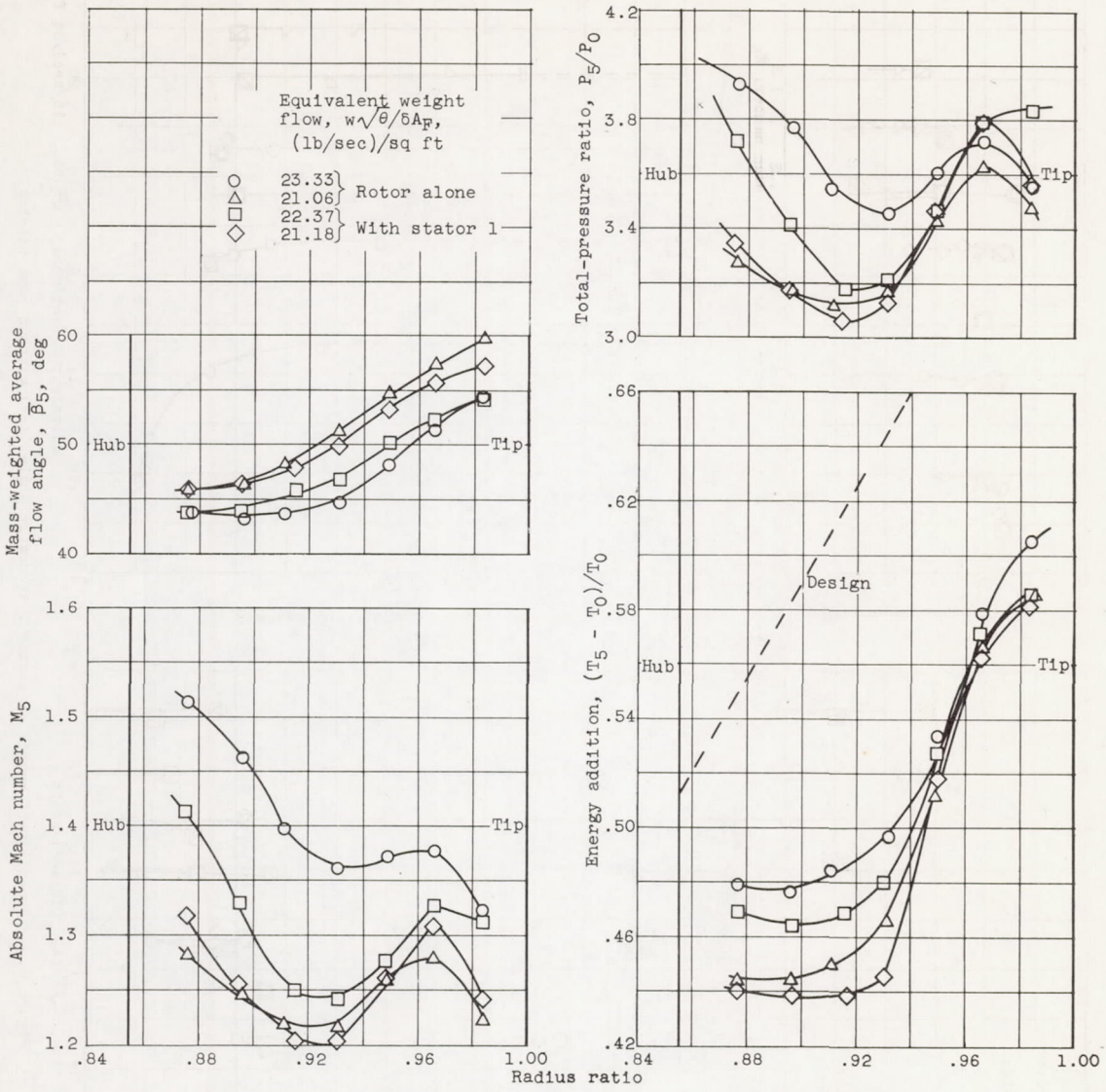

Figure 5. - Flow conditions entering stator at 90-percent design speed

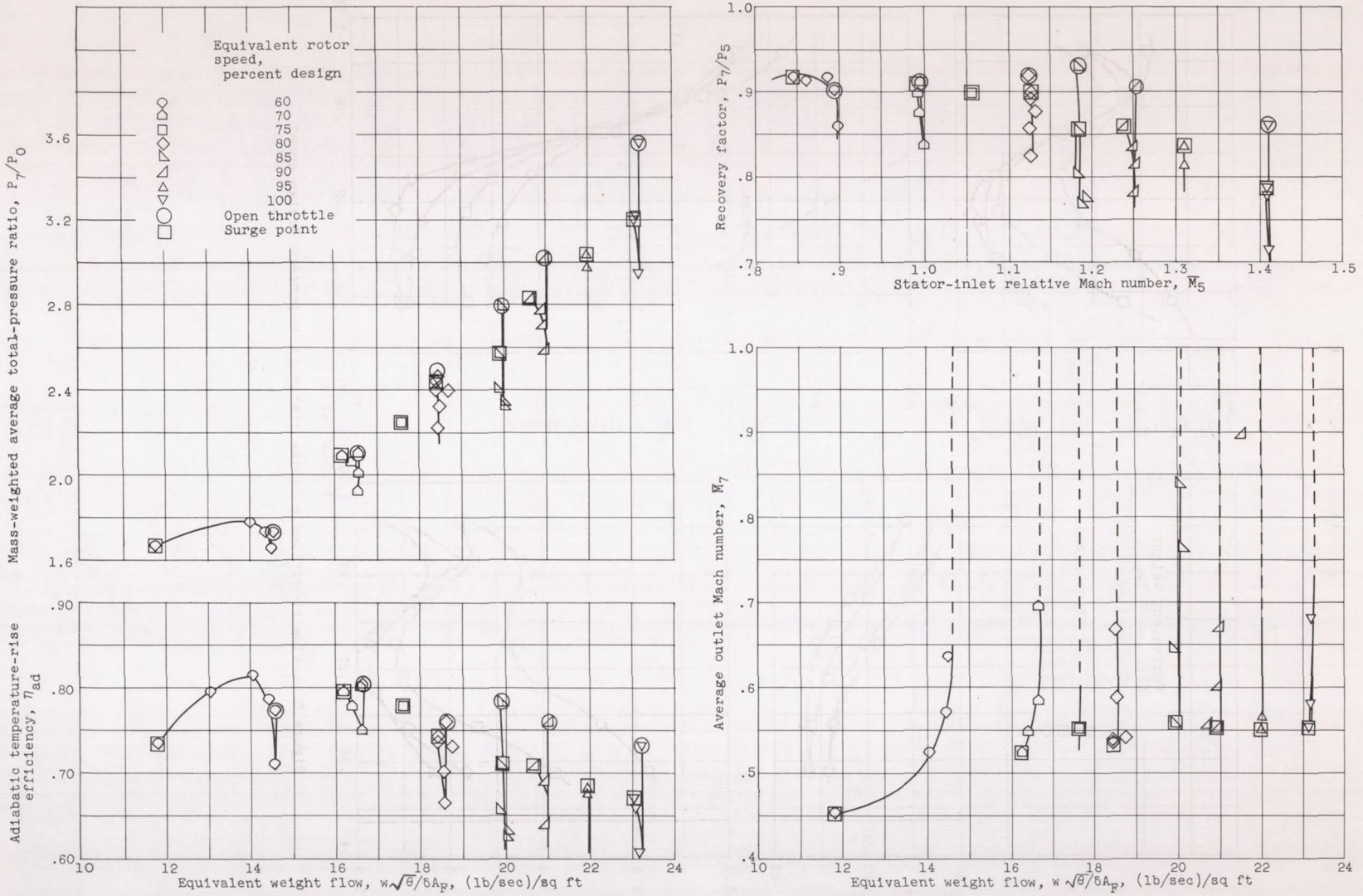

Figure 6. - Over-all performance of stator 1 at design angle (48°) without cone fairing.

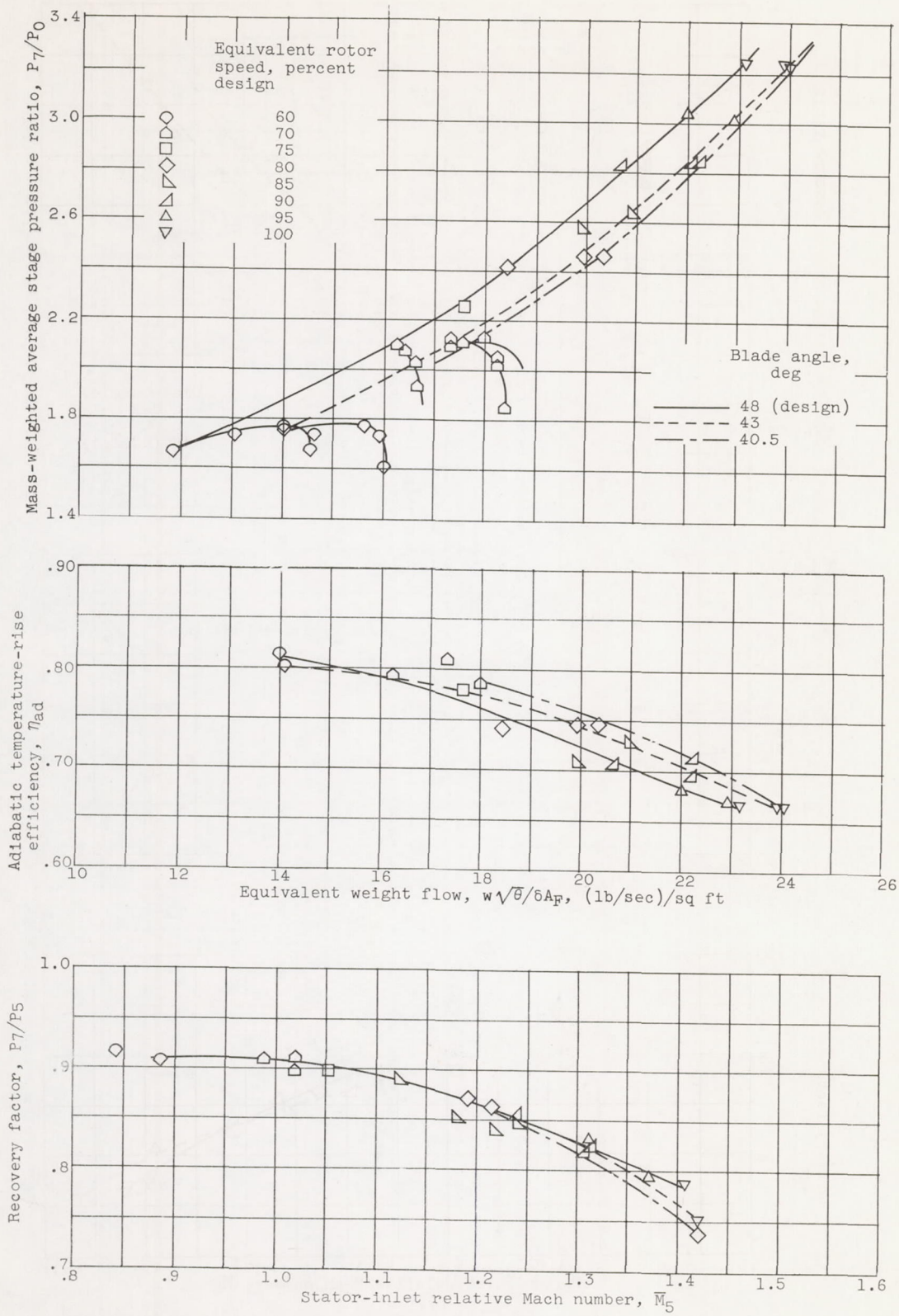

Figure 7. - Effect of resetting blade angles on performance of stator 1 at surge point without cone fairing.

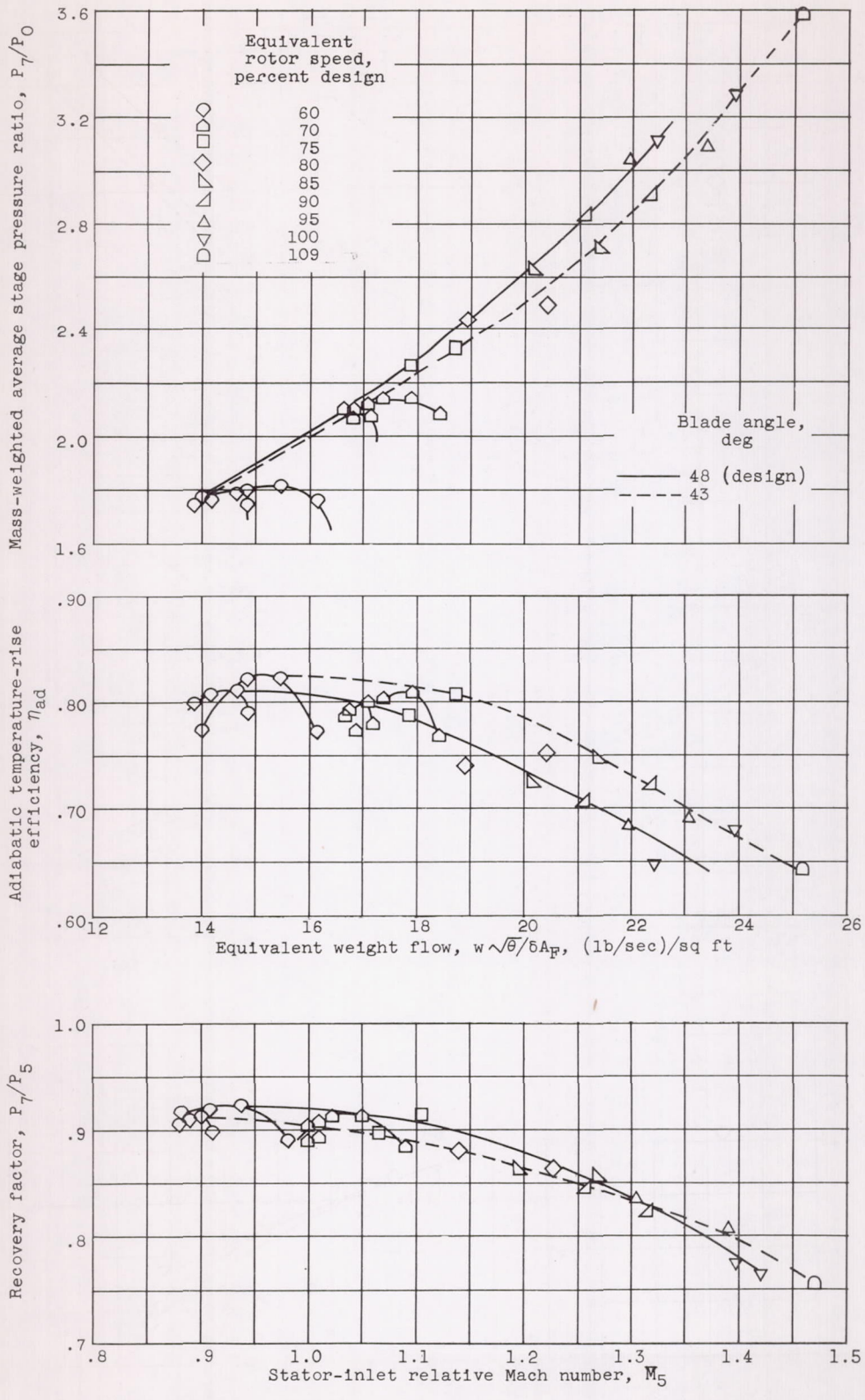

Figure 8. - Performance of stator 1 with cone fairing installed.

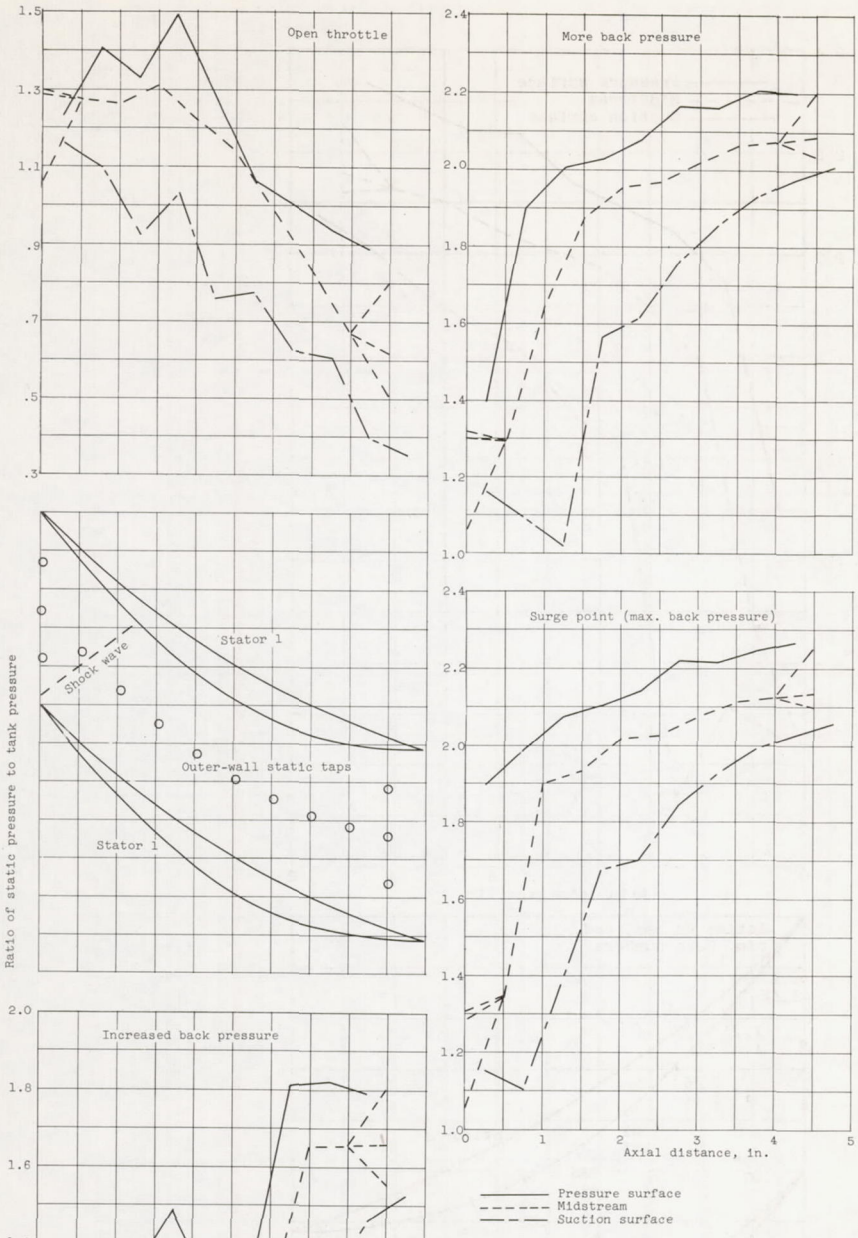

(a) Without cone fairing; blade-angle setting, 48° (design).

Figure 9. - Static pressures on blade surface and outer wall of stator 1 at 90-percent speed.

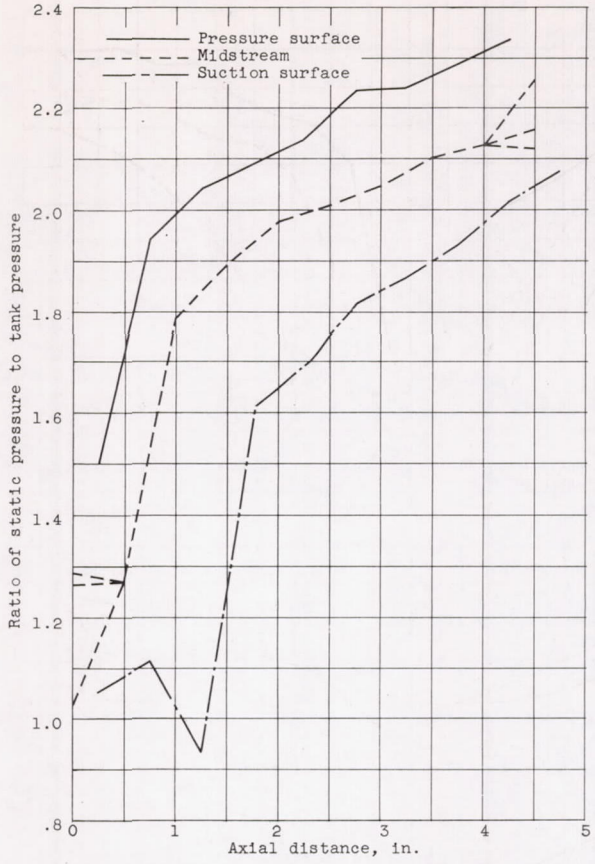

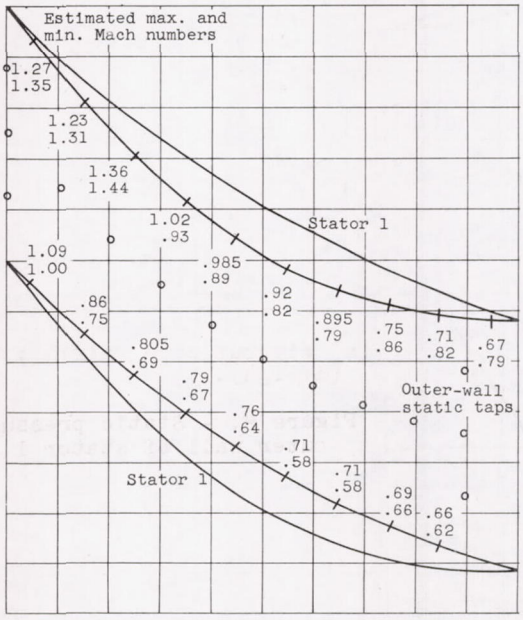

(b) With cone fairing; blade-angle setting, 48° (design); surge point.

Figure 9. - Continued. Static pressures on blade surface and outer wall of stator 1 at 90-percent speed.

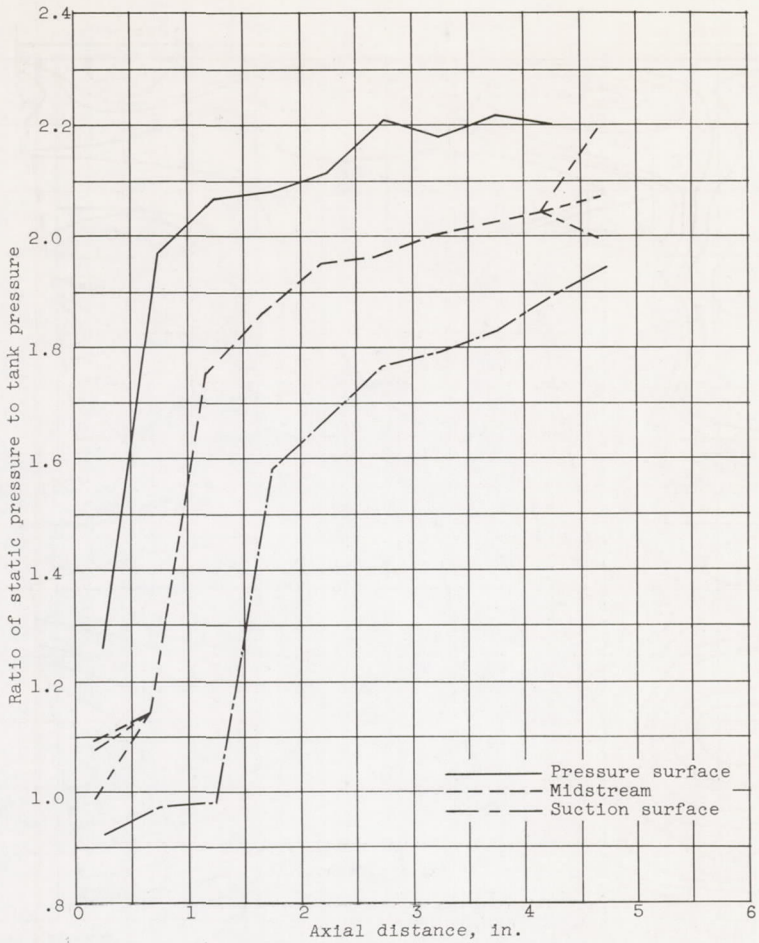

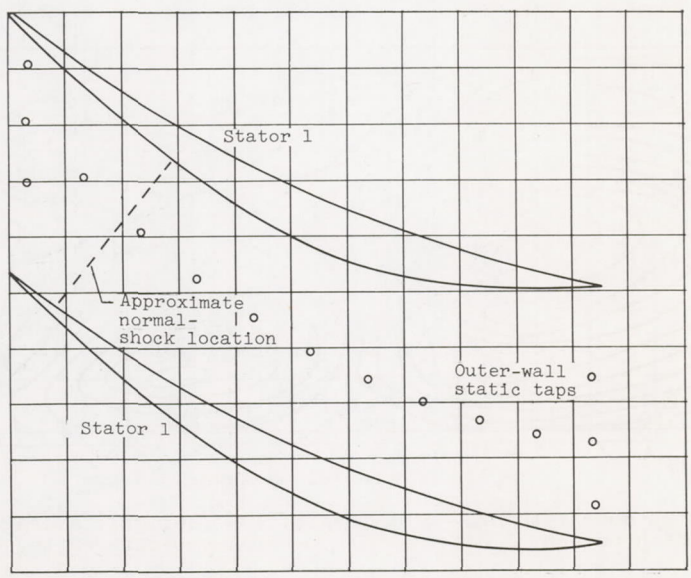

(c) With cone fairing; blade-angle setting, 43°; surge point.

Figure 9. - Concluded. Static pressures on blade surface and outer wall of stator 1 at 90-percent speed.

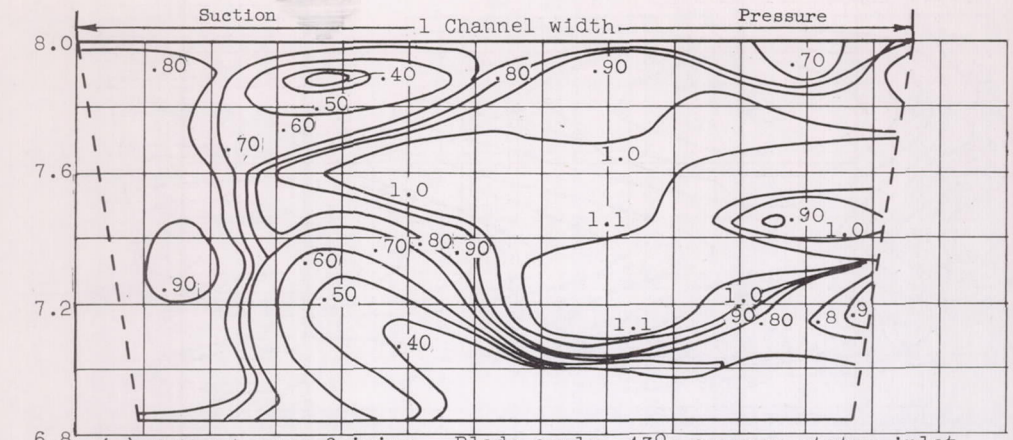

(a) Without cone fairing. Blade angle, 43°; average stator-inlet Mach number, 1.31; static- to total-pressure ratio, 0.356; open throttle.

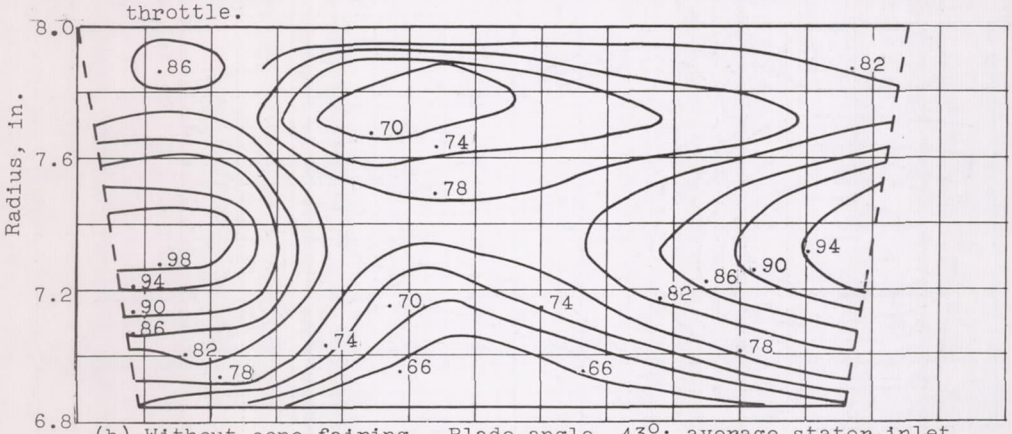

(b) Without cone fairing. Blade angle, 43°; average stator-inlet Mach number, 1.31; static- to total-pressure ratio, 0.356; surge point.

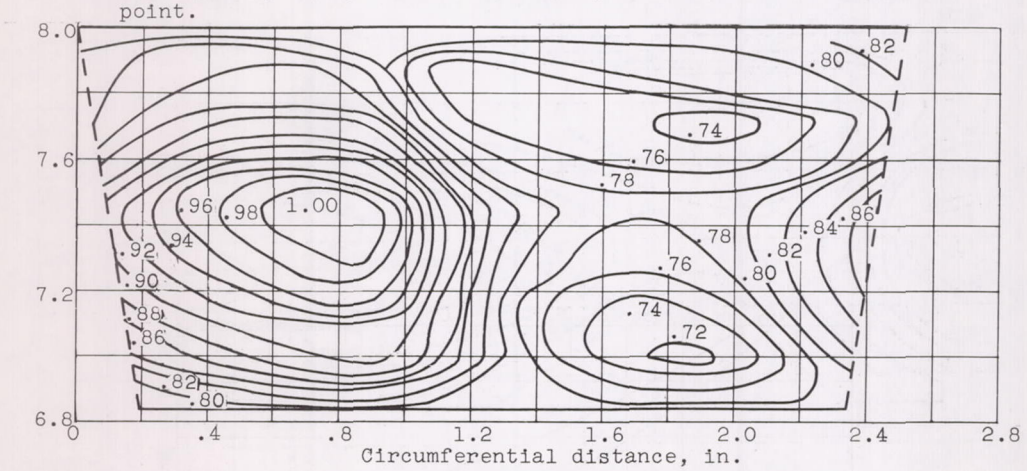

(c) Without cone fairing. Blade angle, 48° (design); average stator-inlet Mach number, 1.24; static- to total-pressure ratio, 0.3912; surge point.

Figure 10. - Profiles of constant recovery factor for stator 1 at 90-percent design speed.

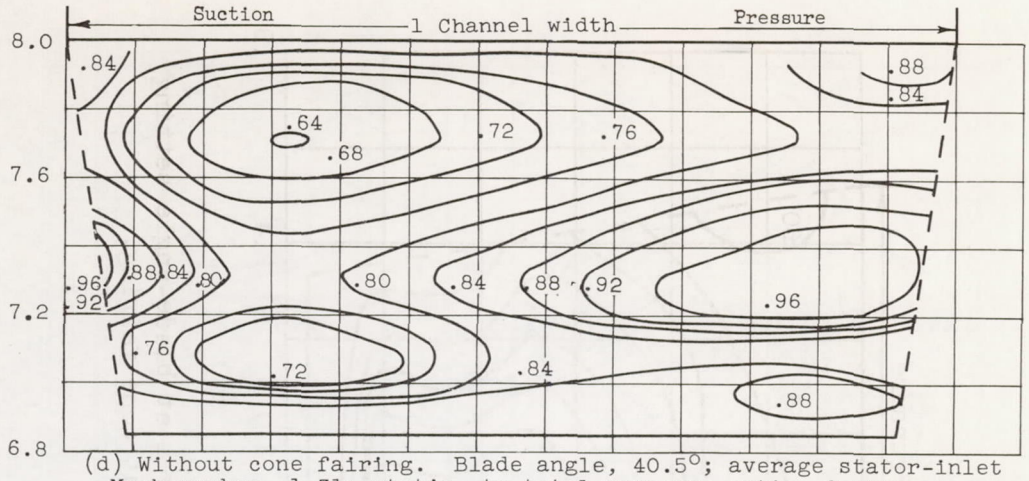

(d) Without cone fairing. Blade angle, 40.5°; average stator-inlet Mach number, 1.31; static- to total-pressure ratio, 0.356; surge point.

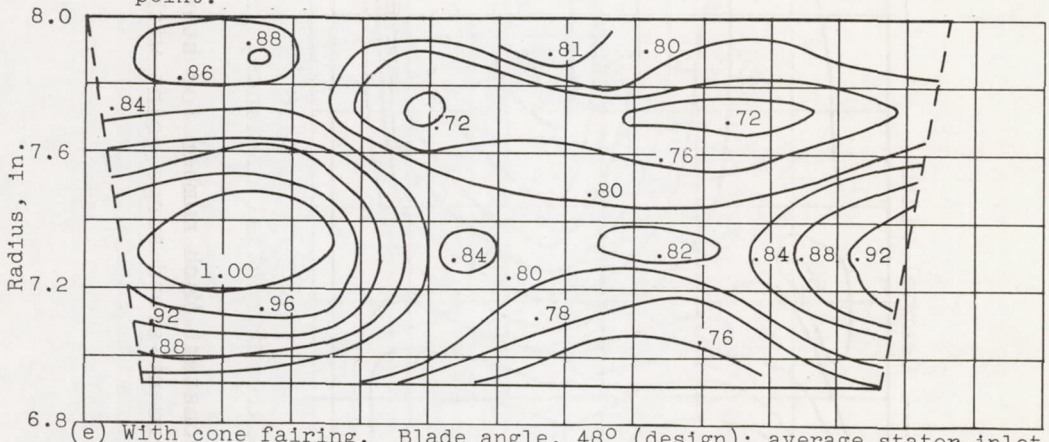

(e) With cone fairing. Blade angle, 48° (design); average stator-inlet Mach number, 1.26; static- to total-pressure ratio, 0.3809; surge point.

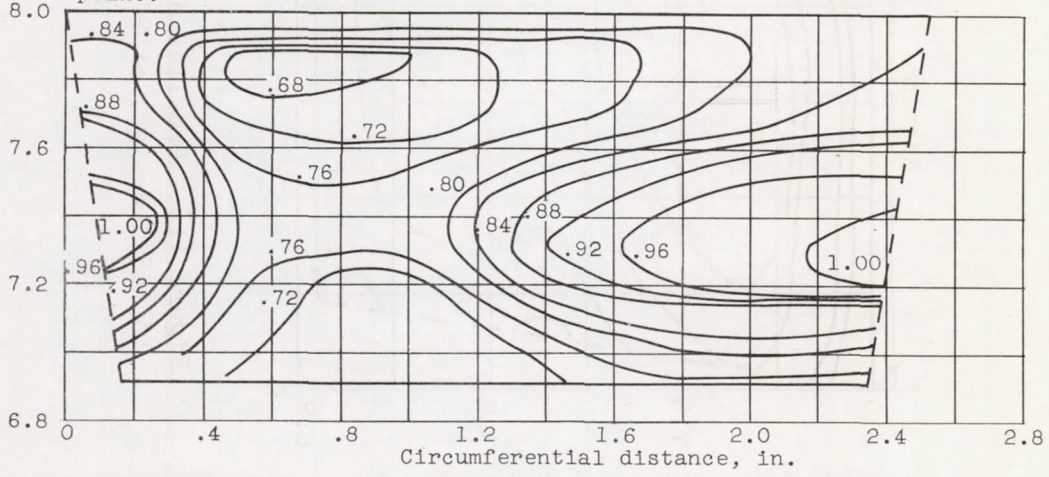

(f) With cone fairing. Blade angle, 43°; average stator-inlet Mach number, 1.32; static- to total-pressure ratio, 0.3512; surge point.

Figure 10. - Concluded. Profiles of constant recovery factor for stator 1 at 90-percent design speed.

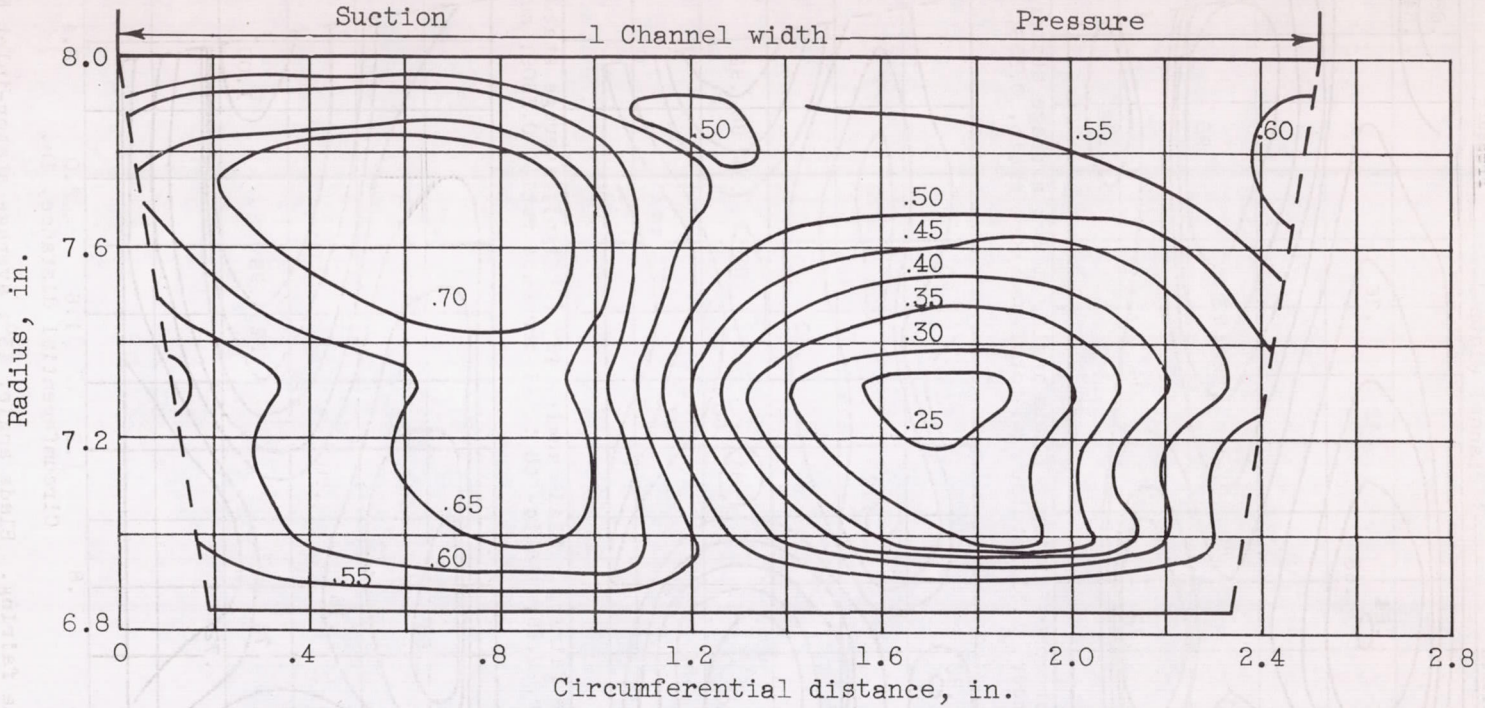

Figure 11. - Profiles of constant Mach number for stator 1 at blade-angle setting of 48° (design) at 90-percent-speed surge point without cone fairing.

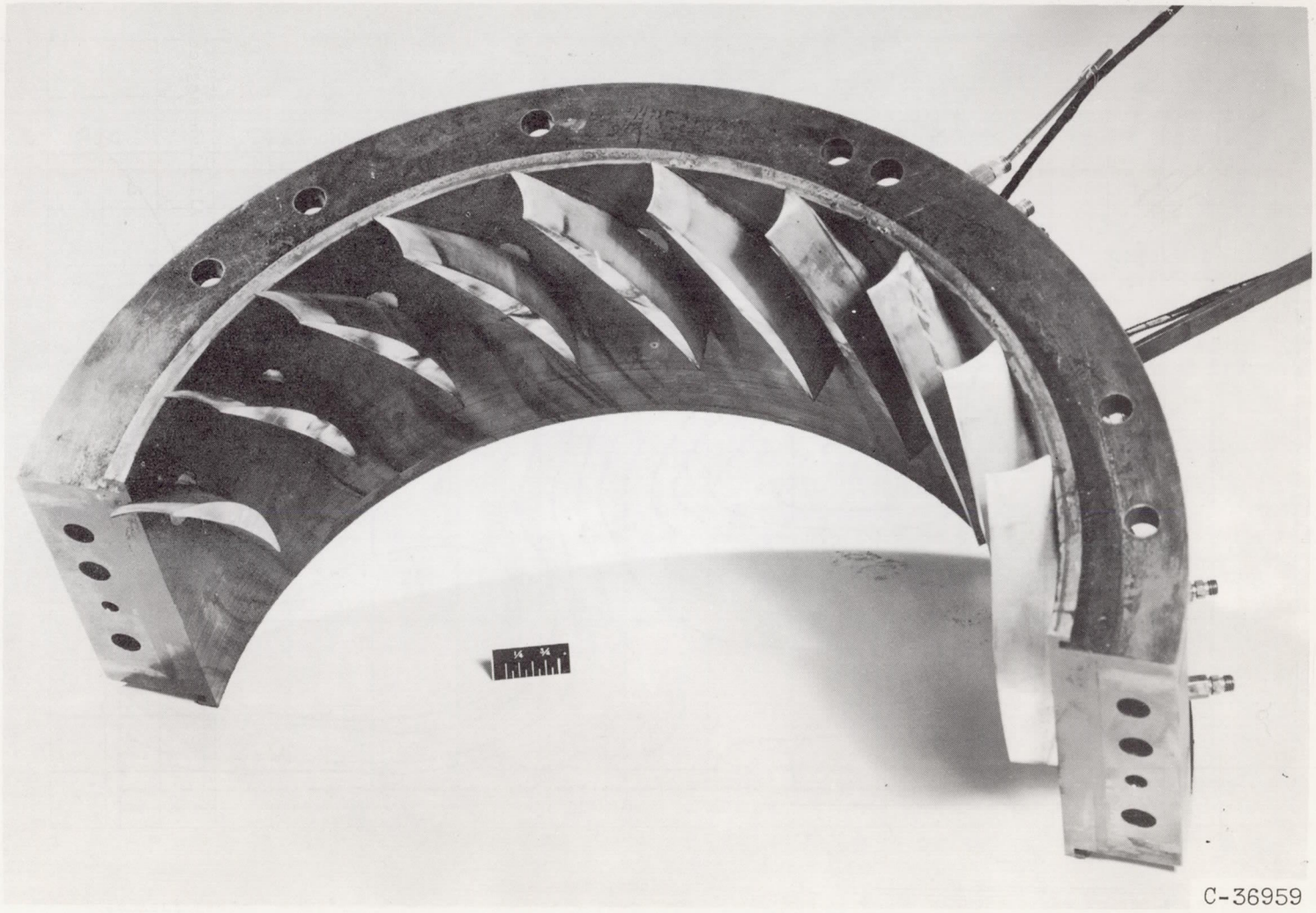

Figure 12. - Photograph of stator 2 at mean-radius blade angle of 43°.

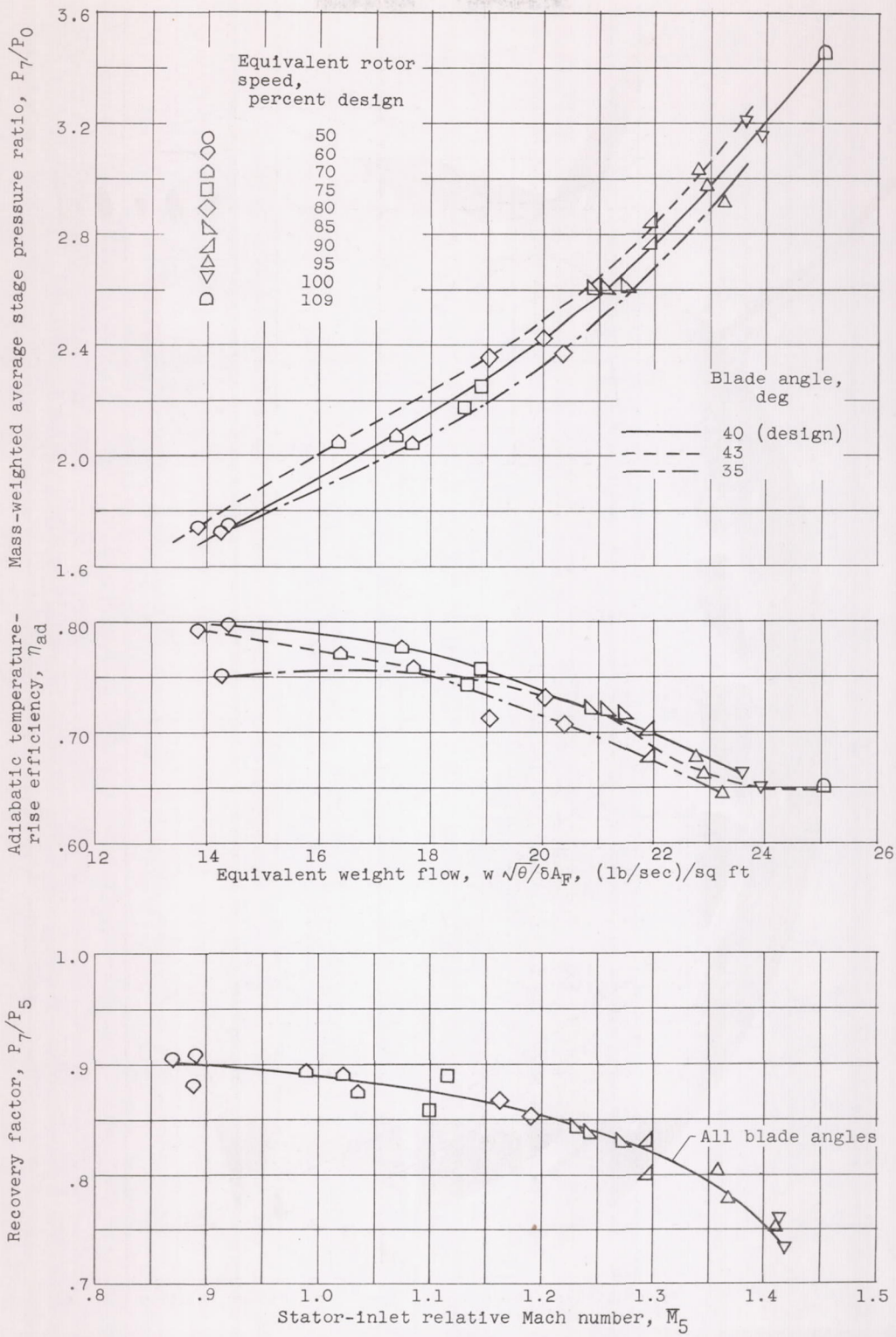

Figure 13. - Performance of stator 2 at blade angles of 40° (design), 35°, and 43° at surge point with cone fairing.

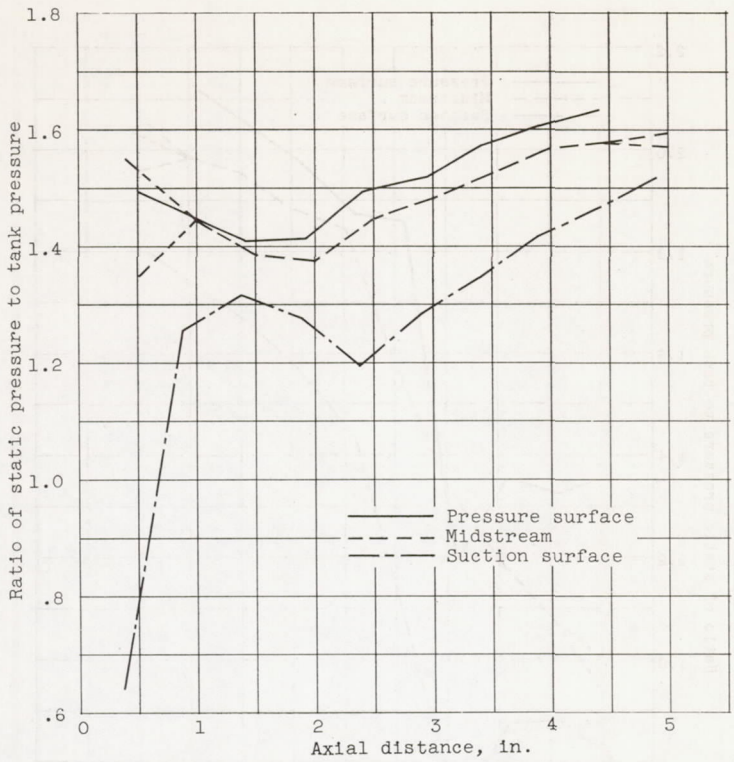

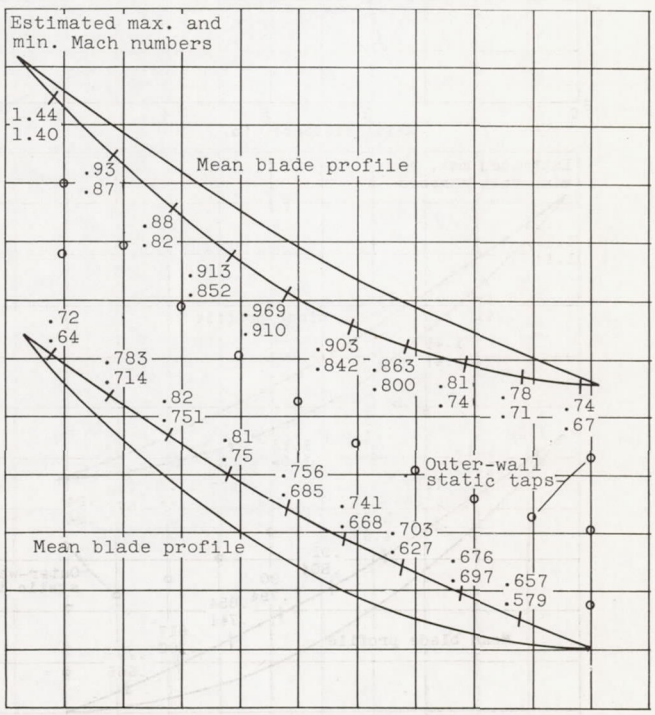

(a) Equivalent rotor speed, 70-percent design; average stator-inlet Mach number, 1.02.

Figure 14. - Static pressures on stator 2 at blade angle of 43° at surge points.

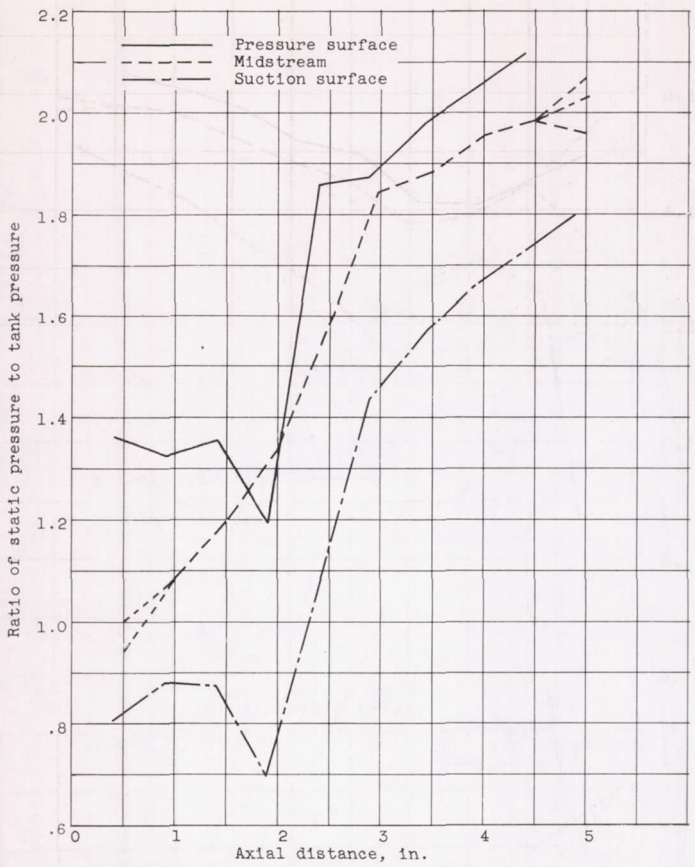

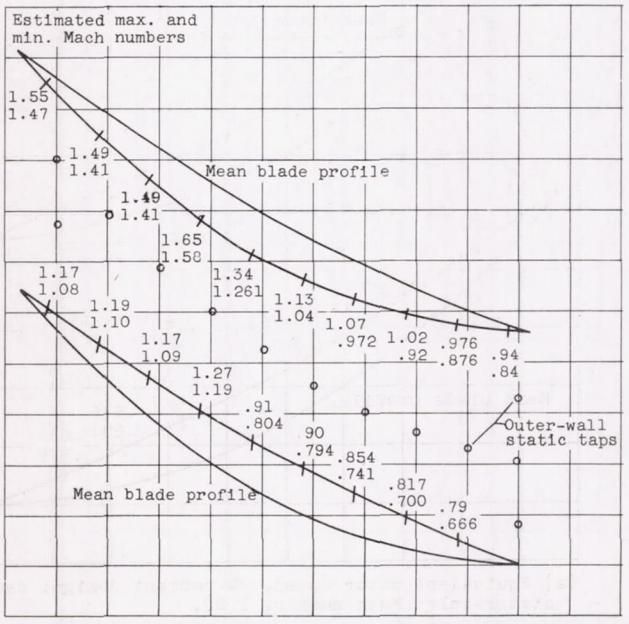

(b) Equivalent rotor speed, 90-percent design; average stator-inlet Mach number, 1.295.

Figure 14. - Concluded. Static pressures on stator 2 at blade angle of 43° at surge points.

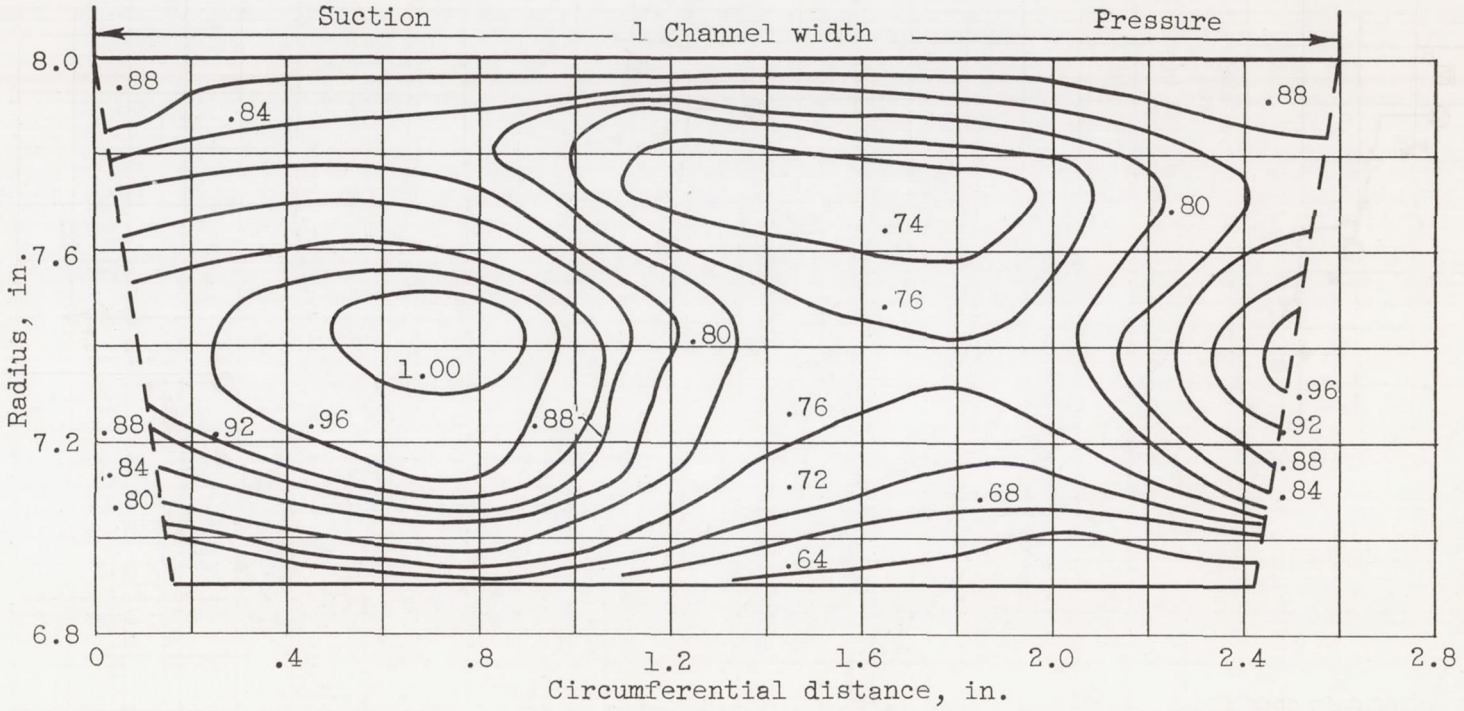

Figure 15. - Profiles of constant recovery factor for stator 2 at blade angle setting of 43° at 90-percent design speed with cone fairing. Average stator-inlet Mach number, 1.295; static- to total-pressure ratio, 0.3658.

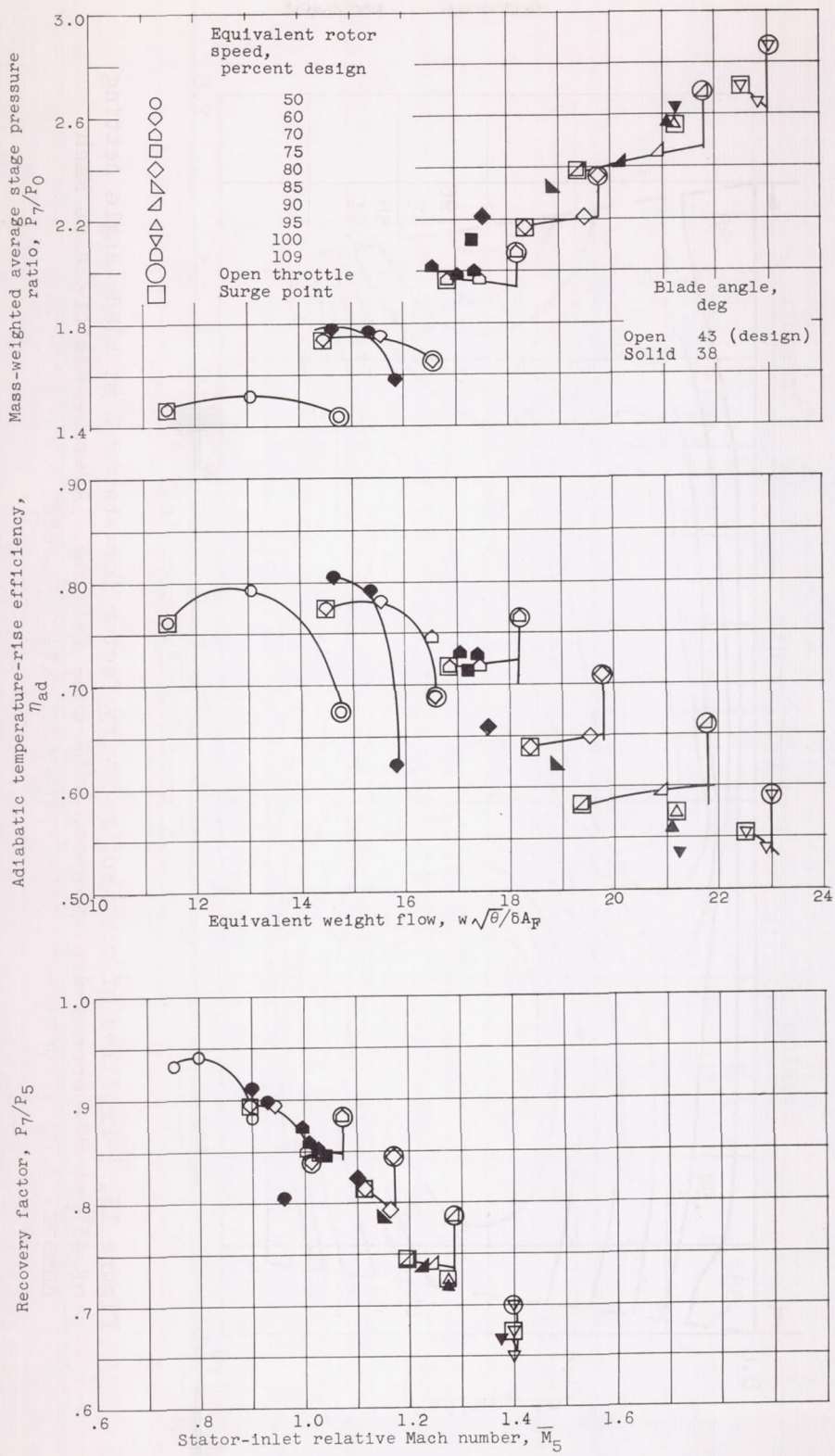

Figure 16. - Performance of stator 3 at blade angles of 43° (design) and 38° with cone fairing.

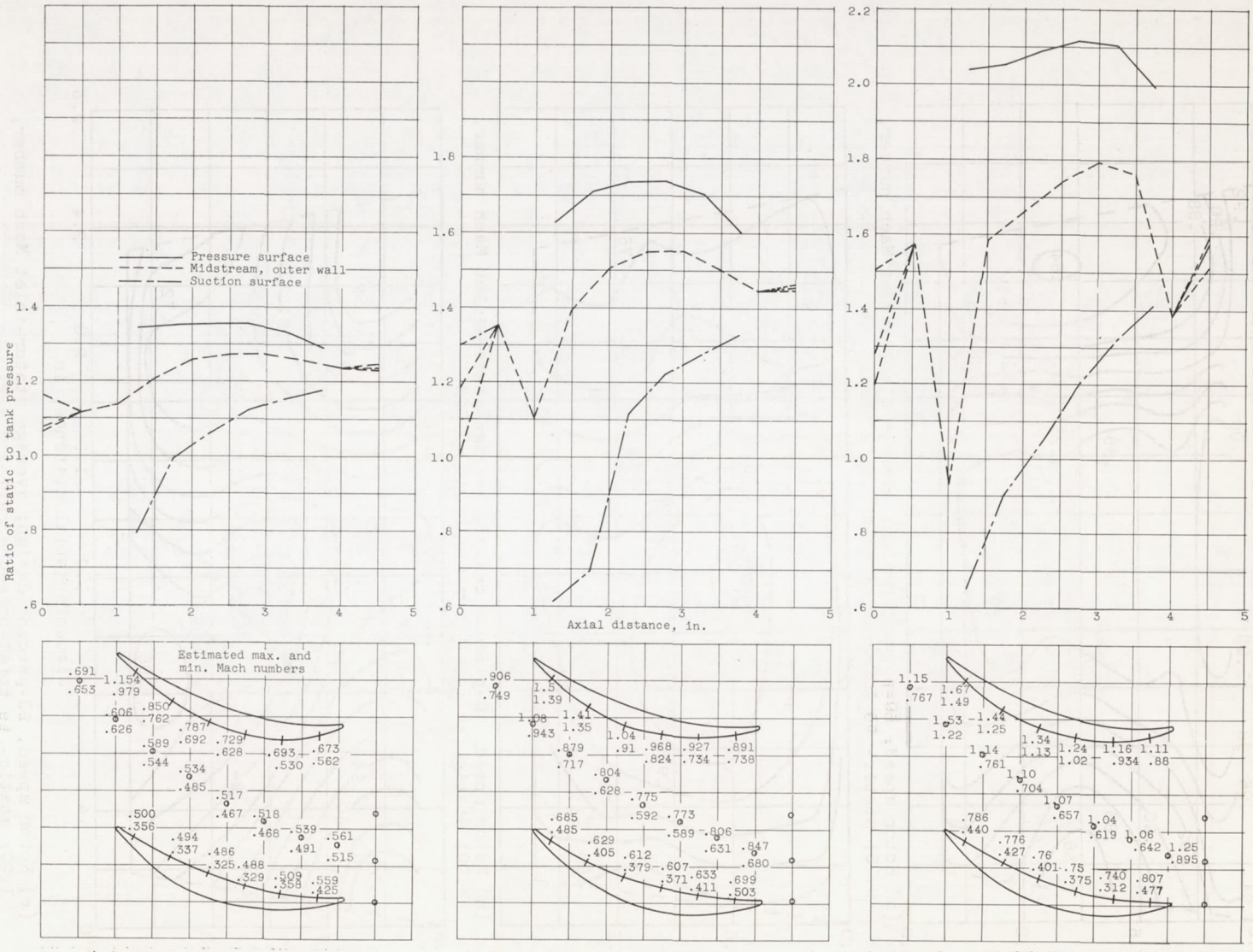

(a) Equivalent rotor speed, 50-percent design.

(b) Equivalent rotor speed, 70-percent design.

(c) Equivalent rotor speed, 90-percent 90-percent design.

Figure 17. - Static pressures on stator 3 at blade angle of 43° (design) at surge points with cone fairing.

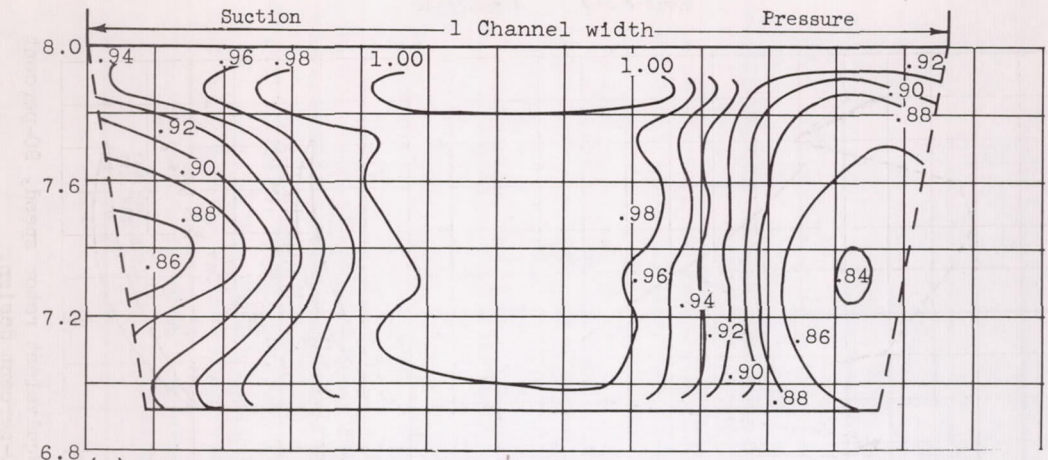

(a) Rotor speed, 50-percent design; average stator-inlet Mach number, 0.75; static- to total-pressure ratio, 0.6886.

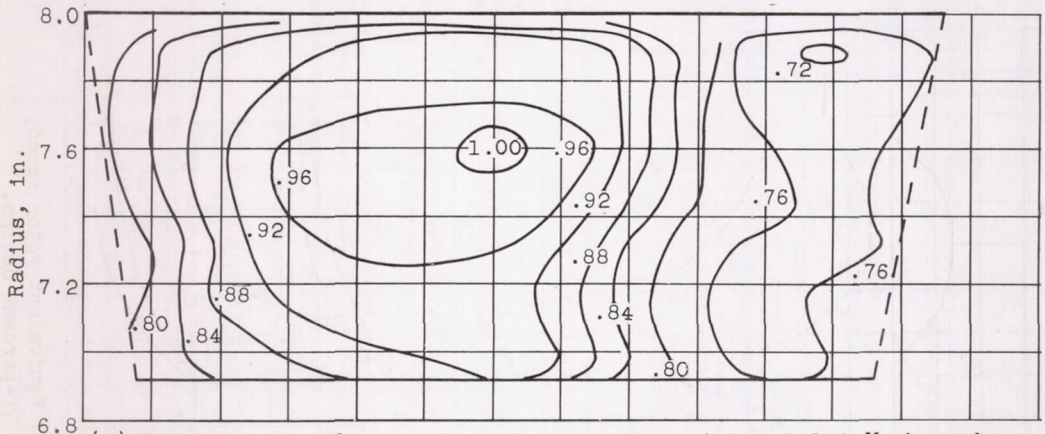

(b) Rotor speed, 70-percent design; average stator-inlet Mach number, 1.00; static- to total-pressure ratio, 0.528.

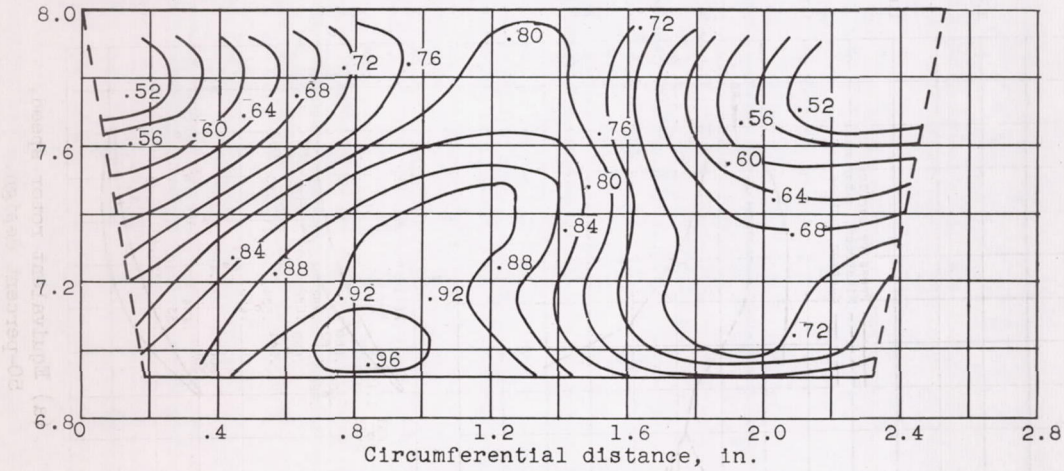

(c) Rotor speed, 90-percent design; average stator-inlet Mach number, 1.20; static- to total-pressure ratio, 0.412.

Figure 18. - Profiles of constant recovery factor for stator 3 with cone fairing at design blade angle of 43°.

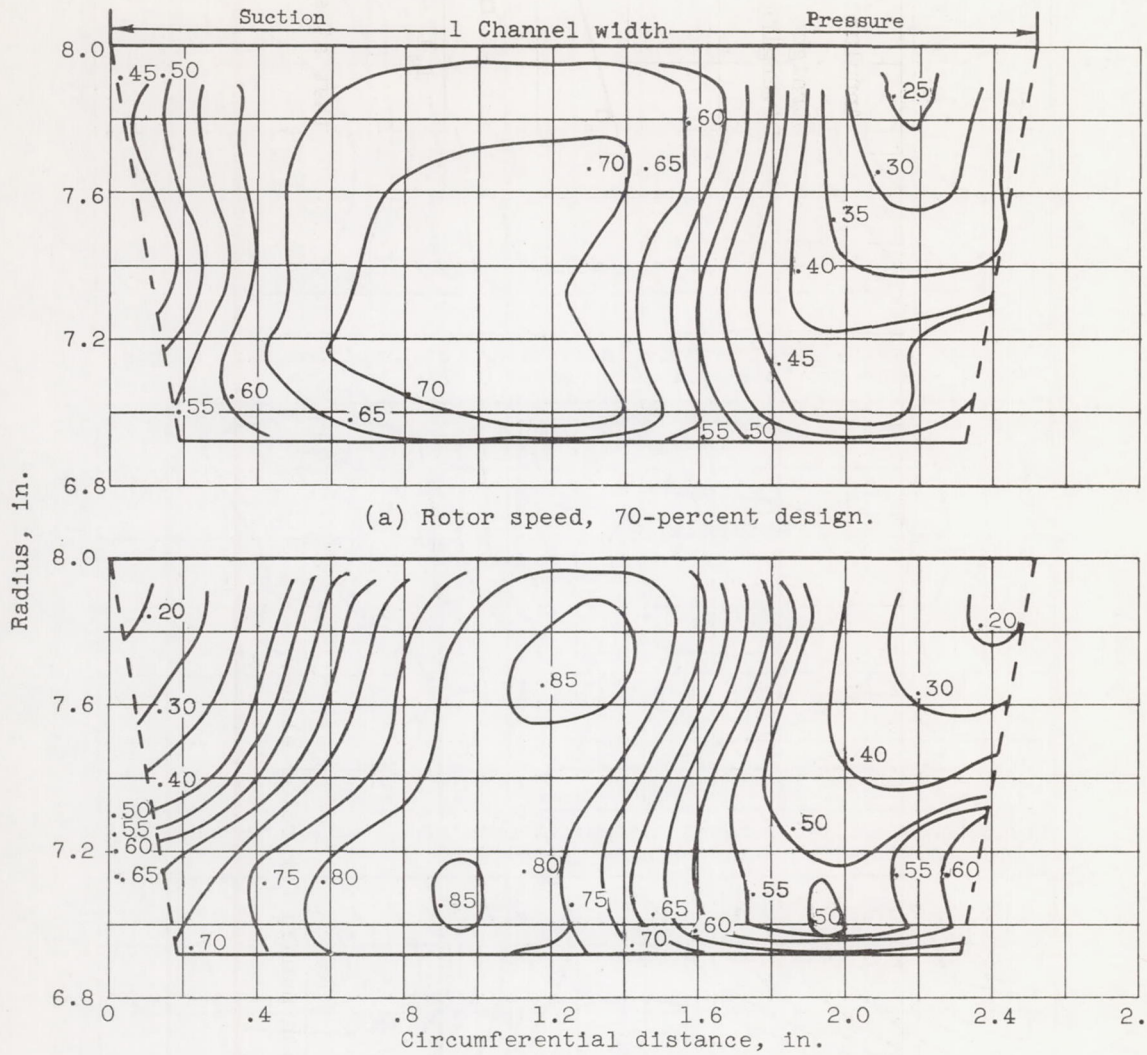

(a) Rotor speed, 70-percent design.

(b) Rotor speed, 90-percent design.

Figure 19. - Profiles of constant Mach number for stator 3 with cone fairing at design blade angle of 43°.

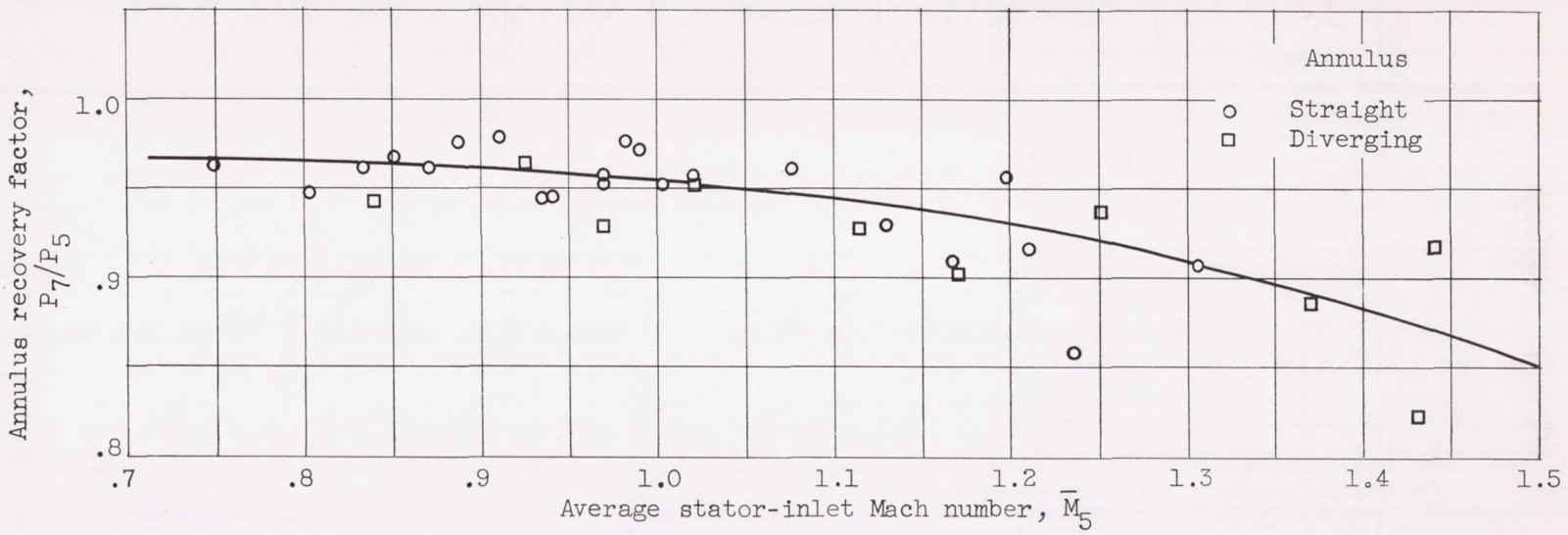

Figure 20. - Variation of ratio of average total-pressure ratio at station 7 to that at station 5 with station 5 Mach number for rotor alone.